

1-LOOP EQUALS TORSION FOR FIBERED 3-MANIFOLDS

NATHAN M. DUNFIELD, STAVROS GAROUFALIDIS, AND SEOKBEOM YOON

ABSTRACT. In earlier work of two of the authors, two 1-loop polynomial invariants of cusped 3-manifolds were constructed using combinatorial data of ideal triangulations, and conjectured to be equal to the \mathbb{C}^2 and the \mathbb{C}^3 -torsion polynomials. Here, we prove this conjecture for all fibered 3-manifolds with toroidal boundary, and we illustrate our theorems with exact computations of the 1-loop and the torsion polynomials. As further evidence for the conjecture, we confirm it for more than 6,600 nonfibered manifolds, and use this data to explore the extent to which the \mathbb{C}^2 -torsion determines the Thurston norm.

CONTENTS

1. Introduction	2
1.1. Acknowledgments.	4
2. Preliminaries	4
2.1. Ptolemy and face equations	4
2.2. Representations	5
2.3. Polynomials	7
2.4. Boundary obstruction classes	8
3. Layered triangulations	9
3.1. Torsion polynomials	10
3.2. Proof of Theorem 1.2	13
4. Examples	15
4.1. The layered triangulation of $m036$	16
4.2. \mathbb{C}^3 -torsion polynomial	17
4.3. \mathbb{C}^2 -torsion polynomial	19
5. Evidence the conjecture holds for nonfibered manifolds	21
5.1. Sample manifolds	21
5.2. Thurston norm and fibering	21
5.3. Checking that 1-loop equals torsion	23
5.4. Lower bounds on the Thurston norm	25
5.5. Labeling the boundary obstruction classes	25
5.6. Sharpness of torsion bounds on the Thurston norm	28
References	28

Date: 31 March 2024.

Key words and phrases. torsion, hyperbolic-torsion, hyperbolic 3-manifold, 1-loop invariant, 1-loop polynomial, pseudo-Anosov homeomorphism, fibered 3-manifold, Ptolemy variables, super-Ptolemy variables, triangulations, taut triangulations, layered triangulations.

1. INTRODUCTION

The torsion polynomials of a hyperbolic 3-manifold are powerful invariants defined from the geometric representation of the manifold. They can be used to certify minimizing properties (i.e., the Thurston norm) of surfaces representing a fixed homology class in the manifold, highlighting a beautiful and interesting connection between the geometry and topology in dimension three.

The \mathbb{C}^n -torsion polynomial $\tau_{n,\rho}(t)$ depends on a 3-manifold M , an integer cohomology class $\alpha \in H^1(M, \mathbb{Z})$ and an $\mathrm{SL}_2(\mathbb{C})$ -representation ρ of $\pi_1(M)$, and it is defined to be the twisted Alexander polynomial associated to the $(n-1)$ -st symmetric power of ρ and α , see for example [Wad94, Kit96]. Here and throughout the paper, a 3-manifold means a compact orientable 3-manifold with toroidal boundary (we do not distinguish the 3-manifold from its interior). One important feature of the torsion polynomials is that they give a bound of the genus of a hyperbolic knot $K \subset S^3$, the smallest genus of an oriented surface spanning K . Precisely, for all $n \geq 2$

$$2 \cdot \text{genus}(K) - 1 \geq \frac{1}{n} \deg \tau_{n,\rho^{\text{geom}}}(t), \quad (1)$$

where ρ^{geom} is an $\mathrm{SL}_2(\mathbb{C})$ -lift of the geometric representation of the knot complement M and $\alpha \in H^1(M, \mathbb{Z})$ is given by the abelianization of $\pi_1(M)$. This inequality appears (and in many cases is shown) to be sharp for $n = 2$, but not for $n = 3$ [AD20, DFJ12].

On the other hand, motivated by Chern–Simons perturbation theory (and the connection between 1-loop perturbation theory and Ray–Singer torsion), Dimofte and the first author [DG13] introduced the 1-loop invariant and showed its topological invariance. The 1-loop invariant is defined from an ideal triangulation of a 3-manifold M along with its gluing equations matrices and a solution to Thurston’s gluing equations, or equivalently, to the Ptolemy equations. A generalization of the 1-loop invariant to a 1-loop polynomial $\delta_{3,c}(t)$ was given in [GYb] using the same ingredients that go into the 1-loop invariant, but with a replacement of the gluing equations matrices with their twisted version that depends on a cohomology class $\alpha \in H^1(M, \mathbb{Z})$. Adding face-variables and face-matrices (which are motivated by super-hyperbolic geometry) to these ingredients, a 1-loop polynomial $\delta_{2,c}(t)$ was recently defined in [GYa]. Here c is a Ptolemy assignment, i.e., a solution to the Ptolemy equations, with or without a boundary obstruction class (see Section 2 for details). Note that a Ptolemy assignment c gives rise to an $\mathrm{SL}_2(\mathbb{C})$ -representation ρ_c of $\pi_1(M)$.

Physics principles predict that the torsion and the 1-loop polynomials should be equal to each other.

Conjecture 1.1. Fix a 3-manifold M , an ideal triangulation \mathcal{T} of M and a cohomology class $\alpha \in H^1(M, \mathbb{Z})$. Then for $n = 2, 3$ and for all Ptolemy assignments c on \mathcal{T} , we have

$$\delta_{n,c}(t) = \tau_{n,\rho_c}(t). \quad (2)$$

Our main result is to prove the above conjecture for 3-manifolds that fiber over the circle. Such a manifold can be written as the mapping torus M_φ of a homeomorphism $\varphi : \Sigma \rightarrow \Sigma$ of a punctured surface Σ , and has a distinguished class $\alpha \in H^1(M, \mathbb{Z})$ induced from the fibration $M_\varphi \rightarrow S^1$. Moreover, using an ideal triangulation on Σ and representing φ by a sequence of 2–2 moves (also known as “flips” [Hat91]), one obtains a layered triangulation \mathcal{T}_φ

of M_φ . Layered triangulations were used by Jorgensen, Floyd and Hatcher to study geometry of once-punctured torus bundles (see [FH82, App.A]), and more recently by [Lac00], whose emphasis was not fibered 3-manifolds, but triangulation methods to certify the Thurston norm.

Theorem 1.2. *When M_φ is a fibered 3-manifold, Equation (2) holds for $n = 2, 3$ and for all Ptolemy assignments c on \mathcal{T}_φ with ρ_c irreducible.*

Let us add some comments to the theorem.

1. The torsion polynomials $\tau_{n,\rho}(t)$ for odd n depend on an $\mathrm{SL}_2(\mathbb{C})$ -representation ρ , and for even n , they depend on the quotient $\mathrm{PSL}_2(\mathbb{C})$ -representation of ρ .
2. When M_φ is hyperbolic, every $\mathrm{SL}_2(\mathbb{C})$ -lift of the geometric representation of M_φ is irreducible, of the form ρ_c and the theorem holds for all such lifts.
3. Theorem 1.2 implies the original 1-loop conjecture of [DG13], namely the equality of the the 1-loop invariant with the \mathbb{C}^3 -torsion (also known as the adjoint Reidemeister torsion), for fibered cusped hyperbolic 3-manifolds. This follows from the fact that the derivatives of the 1-loop polynomial $\delta_{3,c}(t)$ and the \mathbb{C}^3 -torsion polynomial $\tau_{3,\rho}(t)$ at $t = 1$ are the 1-loop invariant and the \mathbb{C}^3 -torsion, respectively [Yam08, GYb].
4. A natural question is an extension of Conjecture 1.1 to all $n \geq 2$. This is possible but rather long and technical, and a sketch of the main ideas involved are given in Section 4 of [GYa]. With additional work, Equation (2) can be proven for all fibered 3-manifolds, but we will not discuss this extension of the theorem here, partly because all known applications to genus detection or to quantum topology involve only the case of $n = 2, 3$.
5. Our 1-loop polynomials are defined by determinantal formulas (see Section 2.3 below), which in the case of fibered 3-manifolds closely resemble the definition of the taut and the veering polynomials of Landry–Minsky–Taylor [LMT], themselves a generalization of the Teichmüller polynomials of McMullen [McM00]; see also Parlak [Par]. This is an intriguing connection, with similarities and differences:
 - (a) all polynomials require an element α of $H^1(M, \mathbb{Z})$,
 - (b) the 1-loop polynomials use arbitrary triangulations whereas the taut/veering polynomials are defined only for taut/veering triangulations,
 - (c) the 1-loop polynomials require a solution to the Ptolemy equations whereas the taut/veering polynomials do not.

Although such a syntactical similarity plays no role in the proof of Theorem 1.2, it is worth pointing it out.

6. Our last comment concerns computational aspects. The torsion and the 1-loop polynomials can be computed using the methods of ideal triangulations developed in SnapPy [CDGW], see [DFJ20]. In Section 5, we check Conjecture 1.1 for more than 6,600 nonfibered 1-cusped hyperbolic 3-manifolds where the all the exact Ptolemy assignments are known by work of Goerner [Goe]. Also in Section 5, we compute the Thurston norm and fibering status for the more than 59,000 manifolds from Burton’s census [Bur]. We use this data to explore whether the analogue of (1) is always sharp for $n = 2$ for more general 3-manifolds. Here, we discovered a new phenomena: whether the inequality is sharp sometimes depends on which $\mathrm{SL}_2(\mathbb{C})$ -lift of the holonomy representation is chosen. When $b_1(M) = 1$ for a 3-manifold M ,

define $x(M) \in \mathbb{Z}_{\geq 0}$ to be the Thurston norm of a generator of $H^1(M; \mathbb{Z})$; one always has $x(M) \geq \frac{1}{2} \deg \tau_{\rho^{\text{geom}}}(t)$ by [DFJ12]. Theorem 5.5 below is a more detailed version of:

Theorem 1.3. *For a sample more than 6,600 nonfibered 1-cusped hyperbolic 3-manifolds with $b_1(M) = 1$, there was always a lift ρ of the holonomy representation where $x(M) = \frac{1}{2} \deg \tau_{2,\rho}(t)$. However, for 50 of these manifolds there was at least one other lift ψ where $x(M) > \frac{1}{2} \deg \tau_{2,\psi}(t)$.*

1.1. Acknowledgments. Yoon wishes to thank Teruaki Kitano and Hyuk Kim for helpful conversations, and Philip Choi and Seonhwa Kim for conducting numerical experiments. Dunfield was partially supported by US NSF grants DMS-1811156 and DMS-2303572 and by a fellowship from the Simons Foundation (673067, Dunfield).

2. PRELIMINARIES

2.1. Ptolemy and face equations. In this section we recall the Ptolemy and face equations associated to ideal triangulations of 3-manifolds.

Let \mathcal{T} be a concrete ideal triangulation of a 3-manifold M , that is, a triangulation such that each tetrahedron comes with a bijection of its vertices with those of the standard 3-simplex. We denote by \mathcal{T}^1 and \mathcal{T}^2 the oriented edges and the unoriented faces of \mathcal{T} , respectively.

A Ptolemy assignment on \mathcal{T} is a map $c : \mathcal{T}^1 \rightarrow \mathbb{C}^*$ satisfying $c(-e) = -c(e)$ for all $e \in \mathcal{T}^1$ and the Ptolemy equation

$$P_{\Delta} : c(e_{01})c(e_{23}) - c(e_{02})c(e_{13}) + c(e_{03})c(e_{12}) = 0 \quad (3)$$

for each tetrahedron Δ of \mathcal{T} . Here e_{ij} is the oriented edge $[i, j]$ of $\Delta = [0, 1, 2, 3]$ as in Figure 1.

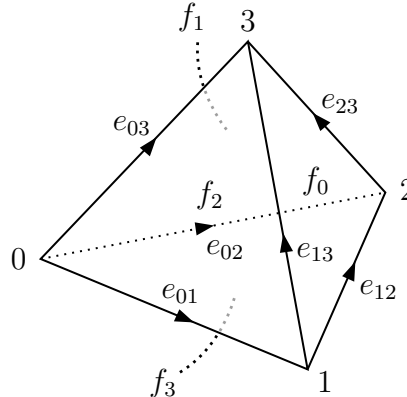


FIGURE 1. Edge and face labels for a tetrahedron.

Since \mathcal{T} has the same number N of tetrahedra as edges, a Ptolemy assignment on \mathcal{T} is represented by an N -tuple (c_1, \dots, c_N) of non-zero complex numbers satisfying N equations. It follows that the set $P_2(\mathcal{T})$ of all Ptolemy assignments on \mathcal{T} is given by

$$P_2(\mathcal{T}) = \{(c_1, \dots, c_N) \in (\mathbb{C}^*)^N \mid P_1 = \dots = P_N = 0\}$$

where $P_1, \dots, P_N \in \mathbb{Z}[c_1, \dots, c_N]$ are the Ptolemy equations for the tetrahedra of \mathcal{T} .

A super-Ptolemy assignment on \mathcal{T} is a Ptolemy assignment $c : \mathcal{T}^1 \rightarrow \mathbb{C}^*$ together with a map $\theta : \mathcal{T}^2 \rightarrow \mathbb{C}$ satisfying one equation, called a face equation, for each face of each tetrahedron Δ of \mathcal{T} :

$$\begin{aligned} E_{\Delta, f_3} &: c(e_{12})\theta(f_0) - c(e_{02})\theta(f_1) + c(e_{01})\theta(f_2) = 0 \\ E_{\Delta, f_2} &: c(e_{13})\theta(f_0) - c(e_{03})\theta(f_1) + c(e_{01})\theta(f_3) = 0 \\ E_{\Delta, f_1} &: c(e_{23})\theta(f_0) - c(e_{03})\theta(f_2) + c(e_{02})\theta(f_3) = 0 \\ E_{\Delta, f_0} &: c(e_{23})\theta(f_1) - c(e_{13})\theta(f_2) + c(e_{12})\theta(f_3) = 0 \end{aligned} \tag{4}$$

Here e_{ij} is the oriented edge $[i, j]$ of $\Delta = [0, 1, 2, 3]$ and f_k is the face of Δ opposite to the vertex k as in Figure 1. Any three equations in (4) are linearly dependent; for instance,

$$c(e_{01})E_{\Delta, f_1} - c(e_{02})E_{\Delta, f_2} + c(e_{03})E_{\Delta, f_3} = 0.$$

It follows that the map θ is only required to satisfy two equations for each tetrahedron, hence total $2N$ equations. Since \mathcal{T} has $2N$ faces, the set $P_{2|1}(\mathcal{T})$ of all super-Ptolemy assignments on \mathcal{T} is given by

$$P_{2|1}(\mathcal{T}) = \{(c_1, \dots, c_N, \theta_1, \dots, \theta_{2N}) \in (\mathbb{C}^*)^N \times \mathbb{C}^{2N} \mid P_1 = \dots = P_N = E_1 = \dots = E_{2N} = 0\}$$

where $E_1, \dots, E_{2N} \in \mathbb{Z}[c_1, \dots, c_N, \theta_1, \dots, \theta_{2N}]$ consist of two face equations of each tetrahedron of \mathcal{T} . Note that a choice of two faces of a tetrahedron is uniquely determined by their common edge, hence the face equations E_1, \dots, E_{2N} are determined by N edges, one in each tetrahedron, possibly with repetition.

2.2. Representations. In this section we briefly recall how Ptolemy and super-Ptolemy assignments lead to representations of $\pi_1(M)$.

A Ptolemy assignment c on \mathcal{T} determines an $\mathrm{SL}_2(\mathbb{C})$ -matrix to every edge of the truncated triangulation of \mathcal{T} as in Figure 2. It is proved in [GTZ15] that these matrices form a 1-cocycle, that is, a representation of the groupoid generated by the 2-skeleton of the truncated triangulation, and hence determine a representation $\rho_c : \pi_1(M) \rightarrow \mathrm{SL}_2(\mathbb{C})$, well-defined up to conjugation. This defines a map

$$P_2(\mathcal{T}) \rightarrow \mathcal{X}(M, \mathrm{SL}_2(\mathbb{C})), \quad c \mapsto \rho_c \tag{5}$$

where

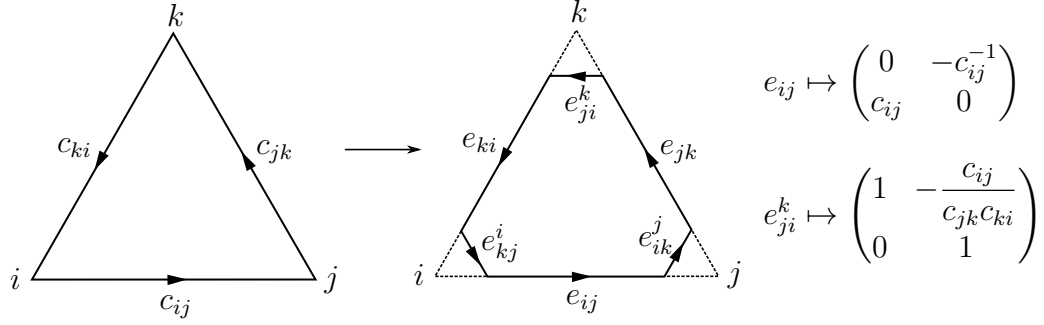
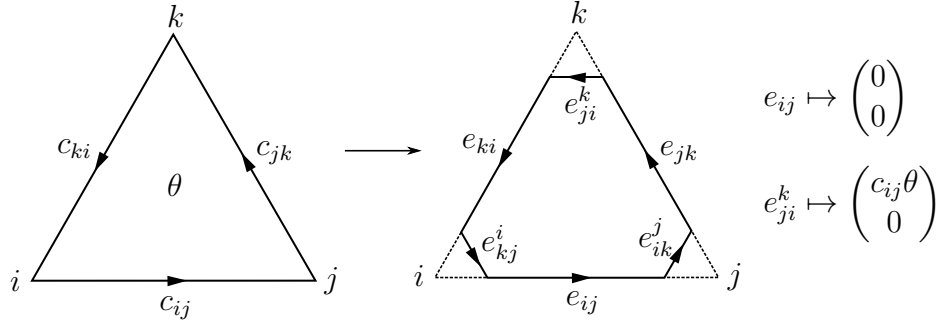
$$\mathcal{X}(M, \mathrm{SL}_2(\mathbb{C})) = \mathrm{Hom}(\pi_1(M), \mathrm{SL}_2(\mathbb{C})) // \mathrm{SL}_2(\mathbb{C}) \tag{6}$$

is the $\mathrm{SL}_2(\mathbb{C})$ -character variety of M . Note that every peripheral curve γ of M satisfies that $\mathrm{tr}(\rho_c(\gamma)) = 2$.

The map θ of a super-Ptolemy assignment (c, θ) on \mathcal{T} allows us to additionally assign a \mathbb{C}^2 -vector to every edge of the truncated triangulation as in Figure 3. These \mathbb{C}^2 -vectors with $\mathrm{SL}_2(\mathbb{C})$ -matrices given in Figure 2 form special affine transformations of \mathbb{C}^2 . It is proved in [GYa] that these affine transformations form a 1-cocycle, hence (up to conjugation) we obtain a representation $\rho_{(c, \theta)} : \pi_1(M) \rightarrow \mathrm{SL}_2(\mathbb{C}) \times \mathbb{C}^2$. This defines a map

$$P_{2|1}(\mathcal{T}) \rightarrow \mathcal{X}(M, \mathrm{SL}_2(\mathbb{C}) \times \mathbb{C}^2), \quad (c, \theta) \mapsto \rho_{(c, \theta)} \tag{7}$$

where $\mathcal{X}(M, \mathrm{SL}_2(\mathbb{C}) \times \mathbb{C}^2)$ is the $(\mathrm{SL}_2(\mathbb{C}) \times \mathbb{C}^2)$ -character variety of M .

FIGURE 2. From Ptolemy assignments to $\mathrm{SL}_2(\mathbb{C})$ -assignments.FIGURE 3. From super-Ptolemy assignments to \mathbb{C}^2 -assignments.

The set $P_2(\mathcal{T})$ admits a $(\mathbb{C}^*)^b$ -action, where b is the number of boundary components of M , defined as follows.

$$(\mathbb{C}^*)^b \times P_2(\mathcal{T}) \rightarrow P_2(\mathcal{T}), \quad (x, c) \mapsto x \cdot c \quad (8)$$

Regarding $x = (x_1, \dots, x_b)$ is assigned to the vertices of \mathcal{T} , $(x \cdot c)(e) := x_i x_j c(e)$ for $e \in \mathcal{T}^1$ where x_i and x_j are assigned to the vertices of e . This action preserves associated $\mathrm{SL}_2(\mathbb{C})$ -representations (see [GTZ15, GGZ15b]). Namely, the map (5) induces

$$P_2(\mathcal{T})/(\mathbb{C}^*)^b \rightarrow \mathcal{X}(M, \mathrm{SL}_2(\mathbb{C})). \quad (9)$$

Although we do not need this in our paper, we remark that the above action extends to $P_{2|1}(\mathcal{T})$ [GYa].

Remark 2.1. Ptolemy and super-Ptolemy assignments also work for punctured surfaces. However, Ptolemy or face equations will not appear, as there is no tetrahedron. Note that an ideal triangulation \mathcal{T} of a punctured surface Σ with Euler characteristic $-n < 0$ has $3n$ edges and $2n$ faces. It follows that we have bijections

$$P_2(\mathcal{T}) \simeq (\mathbb{C}^*)^{3n}, \quad P_{2|1}(\mathcal{T}) \simeq (\mathbb{C}^*)^{3n} \times \mathbb{C}^{2n}. \quad (10)$$

The maps (5) and (7) become

$$(\mathbb{C}^*)^{3n} \rightarrow \mathcal{X}(\Sigma, \mathrm{SL}_2(\mathbb{C})) \quad \text{and} \quad (\mathbb{C}^*)^{3n} \times \mathbb{C}^{2n} \rightarrow \mathcal{X}(\Sigma, \mathrm{SL}_2(\mathbb{C}) \ltimes \mathbb{C}^2) \quad (11)$$

respectively, and the former map induces a map $(\mathbb{C}^*)^{3n}/(\mathbb{C}^*)^p \rightarrow \mathcal{X}(\Sigma, \mathrm{SL}_2(\mathbb{C}))$ as in (9), where p is the number of punctures of Σ .

2.3. Polynomials. In this section we recall the definition of the 1-loop polynomials $\delta_{3,c}(t)$ and $\delta_{2,c}(t)$ associated to a Ptolemy assignment $c \in P_2(\mathcal{T})$, well-defined up to multiplying signs and monomials in t [GYb, Yoo, GYa]. To do so, we fix a cohomology class $\alpha \in H^1(M, \mathbb{Z})$ and denote by \widetilde{M} the infinite cyclic cover of M determined by α and by $\widetilde{\mathcal{T}}$ the ideal triangulation of \widetilde{M} induced from \mathcal{T} .

We fix a lift $\widetilde{\Delta}_j$ of each tetrahedron Δ_j of \mathcal{T} and denote the edges of $\widetilde{\Delta}_1, \dots, \widetilde{\Delta}_N$ in $\widetilde{\mathcal{T}}$ by $\widetilde{e}_1, \dots, \widetilde{e}_I$. The number I of the edges is greater than N , and some of them project down to the same edge in \mathcal{T} . Precisely, there are $I - N$ independent relations of the form

$$\widetilde{e}_i = t^k \cdot \widetilde{e}_j \quad (12)$$

where t is a generator of the deck transformation group \mathbb{Z} of \widetilde{M} .

Assigning a variable \widetilde{c}_i to each edge \widetilde{e}_i for $1 \leq i \leq I$, we obtain N elements

$$\widetilde{P}_1, \dots, \widetilde{P}_N \in \mathbb{Z}[\widetilde{c}_1, \dots, \widetilde{c}_I] \quad (13)$$

from the Ptolemy equations of $\widetilde{\Delta}_1, \dots, \widetilde{\Delta}_N$. Furthermore, since the relation (12) naturally corresponds to an element $\widetilde{c}_i - t^k \widetilde{c}_j$, we obtain additional $I - N$ elements

$$\widetilde{Q}_1, \dots, \widetilde{Q}_{I-N} \in \mathbb{Z}[\widetilde{c}_1, \dots, \widetilde{c}_I][t^{\pm 1}] \quad (14)$$

from the relations on the edges of $\widetilde{\Delta}_1, \dots, \widetilde{\Delta}_N$. Note that a Ptolemy assignment on \mathcal{T} corresponds in an obvious way to an I -tuple $(\widetilde{c}_1, \dots, \widetilde{c}_I)$ of non-zero complex numbers satisfying $\widetilde{P}_1 = \dots = \widetilde{P}_N = 0$ and $\widetilde{Q}_1 = \dots = \widetilde{Q}_{I-N} = 0$ at $t = 1$.

Definition 2.2. Associated to a Ptolemy assignment $c \in P_2(\mathcal{T})$, we define

$$\delta_{3,c}(t) := \pm \left(\prod_e \frac{1}{c(e)} \right) \det \left(\frac{\partial(\widetilde{Q}_1, \dots, \widetilde{Q}_{I-N}, \widetilde{P}_1, \dots, \widetilde{P}_N)}{\partial(\widetilde{c}_1, \dots, \widetilde{c}_I)} \right) \quad (15)$$

where the product is taken over all edges e of \mathcal{T} .

Note that the first $I - N$ rows of the Jacobian matrix in (15) have precisely two non-zero entries, one of which is 1. Therefore, using elementary row operations, one can reduce the size of the Jacobian matrix to N whose entries are given by $\mathbb{Z}[t^{\pm 1}]$ -linear combinations of $c(e)$.

Similarly, we assign a variable $\widetilde{\theta}_j$ to each face of $\widetilde{\Delta}_1, \dots, \widetilde{\Delta}_N$ in $\widetilde{\mathcal{T}}$. The number J of the faces of $\widetilde{\Delta}_1, \dots, \widetilde{\Delta}_N$ in $\widetilde{\mathcal{T}}$ is greater than $2N$, and there are $J - 2N$ independent relations on those faces (as in (12)) which define $J - 2N$ elements

$$\widetilde{F}_1, \dots, \widetilde{F}_{J-2N} \in \mathbb{Z}[\widetilde{\theta}_1, \dots, \widetilde{\theta}_J][t^{\pm 1}] \quad (16)$$

of the form $\widetilde{\theta}_i - t^k \widetilde{\theta}_j$. Also, we have

$$\widetilde{E}_1, \dots, \widetilde{E}_{2N} \in \mathbb{Z}[\widetilde{c}_1, \dots, \widetilde{c}_I][\widetilde{\theta}_1, \dots, \widetilde{\theta}_J] \quad (17)$$

from face equations of $\widetilde{\Delta}_1, \dots, \widetilde{\Delta}_N$, where each tetrahedron contributes two face equations.

Definition 2.3. Associated to a Ptolemy assignment $c \in P_2(\mathcal{T})$, we define

$$\delta_{2,c}(t) := \pm \left(\prod_e \frac{1}{c(e)} \right) \left(\prod_{\Delta} \frac{1}{c(e_{\Delta})} \right) \det \left(\frac{\partial(\tilde{F}_1, \dots, \tilde{F}_{J-2N}, \tilde{E}_1, \dots, \tilde{E}_{2N})}{\partial(\tilde{\theta}_1, \dots, \tilde{\theta}_J)} \right) \quad (18)$$

where the products are taken over all edges e and tetrahedra Δ of \mathcal{T} . Here e_{Δ} is the edge of Δ that determines the two face equations of $\tilde{\Delta}$. Note that entries of the Jacobian matrix in (18) are given by $\mathbb{Z}[t^{\pm 1}]$ -linear combinations of $c(e)$.

For an $\mathrm{SL}_2(\mathbb{C})$ -representation ρ of $\pi_1(M)$ we denote by $\tau_{n,\rho}(t)$ the \mathbb{C}^n -torsion polynomial associated to ρ , i.e., the twisted Alexander polynomial associated to $\mathrm{Sym}^{n-1}(\rho) \otimes \alpha$. See [Wad94] for the precise definition of the twisted Alexander polynomial. Here $\mathrm{Sym}^{n-1}(\rho)$ is the $(n-1)$ -st symmetric power of ρ ; for instance, $\mathrm{Sym}^1(\rho) = \rho$ and $\mathrm{Sym}^2(\rho) = \mathrm{Ad} \circ \rho$. This defines all the invariants that appear in Conjecture 1.1.

As a final remark in this section, if we choose different lifts for the tetrahedra, then the sets I and J above will change, but they will always satisfy $2N < |I| \leq 4N$ and $N < |J| \leq 6N$. If we wish, we may assume that $|I| = 4N$ and $|J| = 6N$ by assigning different variables to all edges and faces (i.e., ignoring edge or face identifications). For instance, if we have N tetrahedra, there are $4N$ faces (ignoring face-pairings) and $2N$ face equations, two from each tetrahedron. We then obtain $2N$ additional equations (of the form $\theta_i - \theta_j t^k = 0$) from $2N$ face-pairings, hence a total of $4N$ equations in $4N$ variables. This $4N \times 4N$ matrix gives the 1-loop \mathbb{C}^2 -polynomial. Note that the last $2N$ rows are of the form $(\dots, 0, 0, 0, 1, 0, \dots, 0, -t^k, 0, 0, 0, \dots)$, so we can apply elementary row operations to reduce the size of this matrix to $2N$.

2.4. Boundary obstruction classes. A solution c to the Ptolemy equations gives rise to an $\mathrm{SL}_2(\mathbb{C})$ -representation ρ_c of $\pi_1(M)$ whose peripheral elements γ satisfy the condition $\mathrm{tr}(\rho_c(\gamma)) = 2$. On the other hand, any $\mathrm{SL}_2(\mathbb{C})$ -lift ρ of the geometric representation of a hyperbolic 3-manifold has a peripheral element γ with $\mathrm{tr}(\rho(\gamma)) = -2$ [Cal06], and hence it is not captured by the Ptolemy equations. To allow such representations, one needs a sign-deformed version of the Ptolemy and face equations (3) and (4). This is a subtle point, often confused in the literature, which we now explain.

It turns out that there are two ways to insert signs to the Ptolemy equation (3), one using an ‘‘obstruction class’’ $\sigma \in H^2(M, \partial M, \mathbb{Z}/2\mathbb{Z}) \simeq H_1(M, \mathbb{Z}/2\mathbb{Z})$ as was done in [GTZ15, GGZ15a, GGZ15b], and a second one using a ‘‘boundary obstruction class’’ $\sigma \in H^1(\partial M, \mathbb{Z}/2\mathbb{Z}) \simeq H_1(\partial M, \mathbb{Z}/2\mathbb{Z})$ introduced in [Yoo19] (unfortunately, a name for these classes was not given there). The two types of obstruction classes are connected by the natural map

$$H_1(\partial M, \mathbb{Z}/2\mathbb{Z}) \rightarrow H_1(M, \mathbb{Z}/2\mathbb{Z}) \quad (19)$$

which sends a boundary obstruction class to an obstruction class.

A solution c to the sign-deformed Ptolemy equations by a boundary obstruction class (resp., by an obstruction class) gives rise to an $\mathrm{SL}_2(\mathbb{C})$ (resp., $\mathrm{PSL}_2(\mathbb{C})$)-representation ρ_c of $\pi_1(M)$ that satisfies the condition $\mathrm{tr}(\rho_c(\gamma)) = \pm 2$ for all peripheral elements γ of $\pi_1(M)$. If c is a solution to the sign-deformed Ptolemy equations by a boundary obstruction class σ and \tilde{c} is the corresponding solution under the obstruction class $\tilde{\sigma}$ of the map (19), then the

$\mathrm{PSL}_2(\mathbb{C})$ -representation $\rho_{\bar{c}}$ is the image of the $\mathrm{SL}_2(\mathbb{C})$ -representation ρ_c under the canonical projection $\mathrm{SL}_2(\mathbb{C}) \rightarrow \mathrm{PSL}_2(\mathbb{C})$.

Coming back to the problem of sign-deforming the Ptolemy and face equations, we will use a cocycle representative of a boundary obstruction class $\sigma \in H^1(\partial M, \mathbb{Z}/2\mathbb{Z})$. Recall that the truncated triangulation of an ideal triangulation \mathcal{T} has short and long edges (see Figure 1) and that the short edges give a triangulation of ∂M . Let σ be a sign-assignment to each short edge such that the product of three signs attached to the boundary of every triangular face is $+1$. Then the Ptolemy equation (3) changes to

$$P_{\Delta} : \quad c(e_{01})c(e_{23}) - \frac{\sigma_{03}^2 \sigma_{12}^3}{\sigma_{03}^1 \sigma_{12}^0} c(e_{02})c(e_{13}) + \frac{\sigma_{02}^3 \sigma_{13}^2}{\sigma_{02}^1 \sigma_{13}^0} c(e_{03})c(e_{12}) = 0. \quad (20)$$

Here $\sigma_{jk}^i \in \{\pm 1\}$ is the sign that σ assigns at the short edge that is near to the vertex i and parallel to the edge $[j, k]$; see Figure 2 or 3. The face equations in (4) change similarly, but now the map θ of a super-Ptolemy assignment (c, θ) is a map from the set of oriented faces of \mathcal{T} , that is, we now distinguish the sides of a face. If we denote by f^{\pm} the sides of a face f , then

$$\theta(f^+) = \sigma_1 \sigma_2 \sigma_3 \theta(f^-) \quad (21)$$

where σ_1, σ_2 , and σ_3 are the signs that σ assigns at the three short edges of the face f . In addition, the face equations in (4) change to

$$\begin{aligned} E_{\Delta, f_3} : \quad & \frac{\sigma_{23}^1}{\sigma_{23}^0} c(e_{12})\theta(f_0^+) - c(e_{02})\theta(f_1^+) + \frac{\sigma_{12}^0}{\sigma_{12}^3} c(e_{01})\theta(f_2^+) = 0 \\ E_{\Delta, f_2} : \quad & c(e_{13})\theta(f_0^+) - \frac{\sigma_{01}^3}{\sigma_{01}^2} c(e_{03})\theta(f_1^+) + \frac{\sigma_{12}^0}{\sigma_{12}^3} c(e_{01})\theta(f_3^+) = 0 \\ E_{\Delta, f_1} : \quad & \frac{\sigma_{03}^1}{\sigma_{03}^2} c(e_{23})\theta(f_0^+) - \frac{\sigma_{01}^3}{\sigma_{01}^2} c(e_{03})\theta(f_2^+) + c(e_{02})\theta(f_3^+) = 0 \\ E_{\Delta, f_0} : \quad & \frac{\sigma_{03}^1}{\sigma_{03}^2} c(e_{23})\theta(f_1^+) - c(e_{13})\theta(f_2^+) + \frac{\sigma_{23}^1}{\sigma_{23}^0} c(e_{12})\theta(f_3^+) = 0 \end{aligned} \quad (22)$$

where f_i^+ is the side of f_i that faces front. Note that Equations (20) and (22) reduce to (3) and (4), respectively, if σ assigns $+1$ to all short edges.

Replacing Equations (3) and (4) by their signed versions (20) and (22) above, one can repeat the definitions of the 1-loop polynomials and their results of Sections 2.2 and 2.3 mutatis-mutandis (see [Yoo19, GYa] for details). Since the choice of the boundary obstruction class will not play any role in the proof of our main theorem 1.2 given in Section 3 below, we will drop the boundary obstruction class σ from the notation of the Ptolemy equations and of the 1-loop polynomials.

3. LAYERED TRIANGULATIONS

In this section we fix a fibered 3-manifold $M = M_{\varphi}$ obtained by the mapping torus of a homeomorphism $\varphi : \Sigma \rightarrow \Sigma$ of a punctured surface. After we choose an ideal triangulation of Σ , and represent φ as a composition of 2–2 moves on triangulations of Σ , we obtain a taut and layered ideal triangulation \mathcal{T}_{φ} of M_{φ} . A detailed description of taut and layered

triangulations is given in Lackenby [Lac00], and a computational approach is given by Bell's program `flipper` [Bel21].

3.1. Torsion polynomials. In this section we give determinantal formulas for the \mathbb{C}^r -torsion polynomials for $r = 2, 3$, adapted to the combinatorics of layered triangulations.

An ideal triangulation of a punctured surface Σ has $3n$ edges and $2n$ triangles where $-n$ is the Euler characteristic of Σ . Hence a super-Ptolemy assignment on (an ideal triangulation of) Σ is given by

$$(c_1, \dots, c_{3n}, \theta_1, \dots, \theta_{2n}) \in (\mathbb{C}^*)^{3n} \times \mathbb{C}^{2n}. \quad (23)$$

Here and throughout the section, all θ_i are assigned to outward oriented faces. Attaching a tetrahedron to a surface creates one edge and two faces. Therefore, we obtain new variables $c_{3n+1}, \dots, c_{3n+N}$ and $\theta_{2n+1}, \dots, \theta_{2n+2N}$ by attaching N tetrahedra on Σ . It follows from Equations (3) and (4) that these new variables are inductively determined by the initial variables given in (23). In addition,

$$\begin{aligned} c_{3n+1}, \dots, c_{3n+N} &\in \mathbb{Q}(c_1, \dots, c_{3n}), \\ \theta_{2n+1}, \dots, \theta_{2n+2N} &\in \mathbb{Q}(c_1, \dots, c_{3n})[\theta_1, \dots, \theta_{2n}] \end{aligned} \quad (24)$$

and each c_i (resp., θ_j) has degree 1 with respect to c_1, \dots, c_{3n} (resp., $\theta_1, \dots, \theta_{2n}$). We denote by $(c'_1, \dots, c'_{3n}, \theta'_1, \dots, \theta'_{2n})$ the super-Ptolemy assignment on the top surface (the surface that we obtain after attaching the tetrahedra) so that a solution to

$$c_i = c'_i \quad \text{and} \quad \theta_j = \theta'_j \quad \text{for} \quad 1 \leq i \leq 3n, \quad 1 \leq j \leq 2n \quad (25)$$

gives a super-Ptolemy assignment on \mathcal{T}_φ , and vice versa.

We now fix a solution to $c_i = c'_i$ for $1 \leq i \leq 3n$, i.e., a Ptolemy assignment c on \mathcal{T}_φ and denote its associated representation by $\rho_c : \pi_1(M_\varphi) \rightarrow \mathrm{SL}_2(\mathbb{C})$.

Lemma 3.1. If ρ_c is irreducible, then so is its restriction $\rho_c|_{\pi_1(\Sigma)}$ to $\pi_1(\Sigma)$.

Proof. Suppose the restriction $\eta = \rho_c|_{\pi_1(\Sigma)}$ is reducible. Then the induced action of $\pi_1(\Sigma)$ on $\mathbb{C}P^1$ (a) acts trivially, (b) has a unique fixed point, or (c) has exactly two fixed points. The first case implies that the image of η is in $\pm I$, hence ρ_c is abelian. This contradicts to the irreducibility of ρ . For the second case, the full group $\pi_1(M)$ must fix the same fixed point, as $\pi_1(\Sigma)$ is a normal subgroup of $\pi_1(M)$. This, again, contradicts to the irreducibility of ρ . The last case implies that up to conjugation the image D of η consists of diagonal matrices. On the other hand, we have $\mathrm{tr} \rho_c(\gamma) = \pm 2$ and $\rho_c(\gamma)D\rho_c(\gamma)^{-1} = D$ for a peripheral curve γ of M . This implies $\rho_c(\gamma) = \pm I$. As $\pi_1(M)$ is generated by $\pi_1(\Sigma)$ and one such γ , this forces ρ_c to be reducible. This completes the proof. \square

Theorem 3.2. The \mathbb{C}^3 -torsion polynomial associated to ρ_c is given by

$$\tau_{3, \rho_c}(t) = \det \left(tI - \frac{\partial(c'_1, \dots, c'_{3n})}{\partial(c_1, \dots, c_{3n})} \right) \quad (26)$$

provided that ρ_c is irreducible.

Proof. Let $\mathcal{X} = \mathcal{X}(\Sigma; \mathrm{SL}_2(\mathbb{C}))$ be the character variety of Σ and $\eta \in \mathcal{X}$ be (the conjugacy class of) the restriction of ρ_c to Σ , which is irreducible due to Lemma 3.1. Let $H_\eta^*(\Sigma; \mathfrak{sl}_2(\mathbb{C}))$

be the twisted cohomology of Σ whose coefficient $\mathfrak{sl}_2(\mathbb{C})$ is twisted by $\text{Ad} \circ \eta$. Since Σ is a punctured surface, $H_\eta^i(\Sigma; \mathfrak{sl}_2(\mathbb{C}))$ is trivial for all $i \geq 2$. Also, since η is irreducible, we have

$$H_\eta^0(\Sigma; \mathfrak{sl}_2(\mathbb{C})) = 0, \quad H_\eta^1(\Sigma; \mathfrak{sl}_2(\mathbb{C})) \simeq T_\eta \mathcal{X} \quad (27)$$

where the latter is Weil's isomorphism [Wei64] (see also [Sik12]). From the usual Mayer-Vietoris sequence for S^1 -fibrations, we obtain (see e.g. [Fri88])

$$\tau_{3,p}(t) = \det(tI - \varphi_{\mathcal{X}}) \quad (28)$$

where $\varphi_{\mathcal{X}} : T_\eta \mathcal{X} \rightarrow T_\eta \mathcal{X}$ is the isomorphism induced by the monodromy $\varphi : \Sigma \rightarrow \Sigma$. Note that the action on \mathcal{X} induced by φ fixes η and its derivative at η is $\varphi_{\mathcal{X}}$.

We first consider the case when φ fixes each puncture of Σ . Let γ_i for $1 \leq i \leq p$ be a small loop that winds around each puncture of Σ . Here p is the number of punctures of Σ . It is clear from Figure 2 that the image of the map $F : (\mathbb{C}^*)^{3n} \rightarrow \mathcal{X}$, sending a Ptolemy assignment on Σ to its associated representation (see Remark 2.1) is contained in

$$\mathcal{Y} = \{\eta' \in \mathcal{X} \mid \text{tr } \eta'(\gamma_1) = \cdots = \text{tr } \eta'(\gamma_p) = 2\} \subset \mathcal{X}. \quad (29)$$

Note that $\eta \in \mathcal{Y}$ and that the image of F is Zariski-open in \mathcal{Y} (see [GTZ15] or [GGZ15b]). The action on \mathcal{X} induced by φ preserves the trace function of each γ_i , hence \mathcal{Y} . This implies that

$$\det(tI - \varphi_{\mathcal{X}}) = (t-1)^p \det(tI - \varphi_{\mathcal{Y}}) \quad (30)$$

where $\varphi_{\mathcal{Y}}$ is the restriction of $\varphi_{\mathcal{X}}$ to $T_\eta \mathcal{Y}$. Note that $\dim T_\eta \mathcal{Y} = \dim T_\eta \mathcal{X} - p = 3n - p$.

Recall that we have two coordinates (c_1, \dots, c_{3n}) and (c'_1, \dots, c'_{3n}) for $(\mathbb{C}^*)^{3n}$. Since we fixed a solution, say c , to $c_i = c'_i$ for $1 \leq i \leq 3n$ with $F(c) = \eta$, we have a commutative diagram for tangent spaces:

$$\begin{array}{ccc} T_c(\mathbb{C}^*)^{3n} & \xrightarrow{\partial c'_i / \partial c_j} & T_c(\mathbb{C}^*)^{3n} \\ \downarrow dF & & \downarrow dF \\ T_\eta \mathcal{Y} & \xrightarrow{\varphi_{\mathcal{Y}}} & T_\eta \mathcal{Y} \end{array} \quad (31)$$

We now fix one puncture of Σ and let $d_i \in \{0, 1, 2\}$ be the number of vertices of the edge c_i that are the chosen puncture. The action (8) on $(\mathbb{C}^*)^{3n}$ says that

$$c'_i(k^{d_1} c_1, \dots, k^{d_{3n}} c_{3n}) = k^{d_i} c'_i(c_1, \dots, c_{3n}), \quad k \in \mathbb{C}^*, \quad 1 \leq i \leq 3n. \quad (32)$$

Here we view c'_i as a function of c_1, \dots, c_{3n} . It follows that the Jacobian $\partial c'_i / \partial c_j$ has an eigenvalue 1 with an eigenvector $(d_1 c_1, \dots, d_{3n} c_{3n})$. Since Σ has p punctures, we obtain p eigenvectors V_1, \dots, V_p with eigenvalues 1. Furthermore, one checks that these eigenvectors are linearly independent from the fact that c_1, \dots, c_{3n} are edges of triangles. On the other hand, the action (8) preserves $\text{SL}_2(\mathbb{C})$ -representations, i.e.,

$$F(c_1, \dots, c_{3n}) = F(k^{d_1} c_1, \dots, k^{d_{3n}} c_{3n}), \quad k \in \mathbb{C}^*, \quad (33)$$

hence the vertical map dF in (31) induces a linear map $T_c((\mathbb{C}^*)^{3n}/(\mathbb{C}^*)^p) \rightarrow T_\eta \mathcal{Y}$ between $(3n-p)$ -dimensional vector spaces. Since the image of F is Zariski-open in \mathcal{Y} , the induced

map is an isomorphism, and thus

$$\det \left(tI - \frac{\partial(c'_1, \dots, c'_{3n})}{\partial(c_1, \dots, c_{3n})} \right) = (t-1)^p \det(tI - \varphi_Y). \quad (34)$$

Then the desired formula (26) follows from (28), (30) and (34).

We now consider the case when φ permutes some punctures of Σ . As the action on \mathcal{X} induced by φ permutes the trace functions of $\gamma_1, \dots, \gamma_p$, we obtain a $p \times p$ -permutation matrix P with

$$\det(tI - \varphi_X) = \det(tI - P) \det(tI - \varphi_Y) \quad (35)$$

instead of Equation (30). Similarly, the vectors V_1, \dots, V_p would be no longer eigenvectors, but the Jacobian $\partial c'_i / \partial c_j$ permutes them with the same permutation matrix P . Namely,

$$\det \left(tI - \frac{\partial(c'_1, \dots, c'_{3n})}{\partial(c_1, \dots, c_{3n})} \right) = \det(tI - P) \det(tI - \varphi_Y). \quad (36)$$

Combining the above two equations, we obtain the desired formula (37). \square

Theorem 3.3. *The \mathbb{C}^2 -torsion polynomial associated to ρ_c is given by*

$$\tau_{2, \rho_c}(t) = \det \left(tI - \frac{\partial(\theta'_1, \dots, \theta'_{2n})}{\partial(\theta_1, \dots, \theta_{2n})} \right) \quad (37)$$

provided that ρ_c is irreducible.

Note that θ'_i is linear in $\theta_1, \dots, \theta_{2n}$, hence $\partial \theta'_i / \partial \theta_j$ is in $\mathbb{Q}(c_1, \dots, c_{3n})$; in particular, the determinant in (37) only depends on the Ptolemy assignment.

Proof. Let $\mathcal{X} = \mathcal{X}(\Sigma; \mathrm{SL}_2(\mathbb{C}))$ be the character variety of Σ and $\eta \in \mathcal{X}$ be (the conjugacy class of) the restriction of ρ_c to Σ , which is irreducible due to Lemma 3.1. Let $H_\eta^*(\Sigma; \mathbb{C}^2)$ be the twisted cohomology of Σ whose coefficient \mathbb{C}^2 is twisted by η . Since Σ is a punctured surface and η is irreducible, $H_\eta^i(\Sigma; \mathbb{C}^2)$ is trivial for all i but $i = 1$. We first claim that

$$H_\eta^1(\Sigma; \mathbb{C}^2) \simeq T_\eta \mathcal{Z} \quad \text{for } \mathcal{Z} := p^{-1}(\eta) \quad (38)$$

where $p : \mathcal{X}(\Sigma; \mathrm{SL}_2(\mathbb{C}) \times \mathbb{C}^2) \rightarrow \mathcal{X}$ is the natural projection map. Here we identify η with $(\eta, 0) : \pi_1(\Sigma) \rightarrow \mathrm{SL}_2(\mathbb{C}) \times \mathbb{C}^2$.

An element of \mathcal{Z} is represented by a pair (η, v) where $v : \pi_1(\Sigma) \rightarrow \mathbb{C}^2$ is a 1-cocycle, i.e., a map satisfying

$$v(ab) = v(a) + \eta(a)v(b) \quad \text{for all } a, b \in \pi_1(\Sigma). \quad (39)$$

As the condition (39) is linear in v , a vector in $T_\eta \mathcal{Z}$ is also represented by a 1-cocycle. We define a map from $T_\eta \mathcal{Z}$ to $H_\eta^1(\Sigma; \mathbb{C}^2)$ naturally by sending a 1-cocycle to its class in the first cohomology. Then a routine computation shows that this map is an isomorphism. Note that $\dim T_\eta \mathcal{Z} = \dim H^1(\Sigma; \mathbb{C}^2) = 2n$.

From the usual Mayer-Vietoris sequence for S^1 -fibrations, we obtain (see e.g. [Fri88])

$$\tau_{2, \rho}(t) = \det(tI - \varphi_{\mathcal{Z}}) \quad (40)$$

where $\varphi_{\mathcal{Z}} : T_\eta \mathcal{Z} \rightarrow T_\eta \mathcal{Z}$ is the isomorphism induced by the monodromy φ . Note that φ acts on \mathcal{X} fixing η , hence it induces an action on \mathcal{Z} , whose derivative at η is $\varphi_{\mathcal{Z}}$.

Recall that we have a fixed Ptolemy assignment, say c , on Σ whose associated representation is η . Let $G : \mathbb{C}^{2n} \rightarrow \mathcal{Z}$ be a map sending $\theta \in \mathbb{C}^{2n}$ to the representation associated to the super-Ptolemy assignment (c, θ) (see Remark 2.1). It is clear that the image of G is contained in \mathcal{Z} with $G(0) = \eta$. In addition, it is proved in [GYa] that the image of G is Zariski-open in \mathcal{Z} . On the other hand, we obtain a commutative diagram for tangent spaces from two coordinates $(\theta_1, \dots, \theta_{2n})$ and $(\theta'_1, \dots, \theta'_{2n})$ for \mathbb{C}^{2n} :

$$\begin{array}{ccc} T_0\mathbb{C}^{2n} & \xrightarrow{\partial\theta'_i/\partial\theta_j} & T_0\mathbb{C}^{2n} \\ \downarrow dG & & \downarrow dG \\ T_\eta\mathcal{Z} & \xrightarrow{\varphi_{\mathcal{Z}}} & T_\eta\mathcal{Z} \end{array} \quad (41)$$

Then the desired formula (37) follows from (40) and (41). \square

3.2. Proof of Theorem 1.2. In this section we compare the formulas for the torsion polynomials given in Theorems 3.2 and 3.3 with analogous formulas for the 1-loop polynomials to deduce Theorem 1.2.

Claim 1. Equation (2) holds for $n = 3$ and for all Ptolemy assignments c on \mathcal{T}_φ with ρ_c irreducible.

Proof. We label the edges of \mathcal{T}_φ as in Section 3.1: the edges of Σ are labeled with c_1, \dots, c_{3n} and the new edge created when we attach the i -th tetrahedron Δ_i is labeled by c_{3n+i} for $1 \leq i \leq N$. Note that some edges have multiple labels. The Ptolemy equation P_i of Δ_i is written as

$$P_i : c_{T(i)}c_{B(i)} - c_{E_1(i)}c_{E_2(i)} + c_{E_3(i)}c_{E_4(i)} = 0 \quad (42)$$

where $c_{T(i)}$ and $c_{B(i)}$ are the top and bottom edges and $c_{E_1(i)}, \dots, c_{E_4(i)}$ are the equatorial edges of Δ_i . Note that $T(i) = 3n + i$ and $B(i), E_1(i), \dots, E_4(i) \leq 3n + i - 1$ and that $\{c_{B(1)}, \dots, c_{B(N)}\}$ is the edge set of \mathcal{T}_φ . Then, as we explained in Section 2.3, the 1-loop polynomial $\delta_{3,c}(t)$ is given by

$$\delta_{3,c}(t) = \left(\prod_{i=1}^N \frac{1}{c_{B(i)}} \right) \det \left(\frac{\partial(Q_1, \dots, Q_{3n}, P_1, \dots, P_N)}{\partial(c_1, \dots, c_{3n+N})} \right) \quad (43)$$

where $Q_i = tc_i - c'_i$ for $1 \leq i \leq 3n$ where c'_i is the Ptolemy variable on the top surface at the same position as c_i . Letting $P'_i = P_i/c_{B(i)}$ for $1 \leq i \leq N$, we have

$$\delta_{3,c}(t) = \det \left(\frac{\partial(Q_1, \dots, Q_{3n}, P'_1, \dots, P'_N)}{\partial(c_1, \dots, c_{3n+N})} \right) = \det \left(\begin{array}{cc|cc} t & & * & \\ & \ddots & & * \\ * & & t & \\ \hline & * & & 1 \\ & & & 0 \\ & & & * \\ & & & 1 \end{array} \right). \quad (44)$$

Using a determinant formula for block matrices

$$\det \left(\begin{array}{c|c} A & b \\ \hline c & 1 \end{array} \right) = \det(A - bc), \quad (45)$$

the determinant in (44) equals to

$$\det \left(\frac{\partial(Q_1, \dots, Q_{3n}, P'_1, \dots, P'_{N-1})}{\partial(c_1, \dots, c_{3n+N-1})} - \begin{pmatrix} \frac{\partial Q_1}{\partial c_{3n+N}} \\ \vdots \\ \frac{\partial Q_{3n}}{\partial c_{3n+N}} \\ 0 \\ \vdots \\ 0 \end{pmatrix} \begin{pmatrix} \frac{\partial P'_N}{\partial c_1} & \dots & \frac{\partial P'_N}{\partial c_{3n+N-1}} \end{pmatrix} \right). \quad (46)$$

On the other hand, solving the equation $P'_N = 0$ gives

$$c_{3n+N} = \frac{c_{E_1(N)}c_{E_2(N)} - c_{E_3(N)}c_{E_4(N)}}{c_{B(N)}}, \quad (47)$$

hence $\partial P'_N / \partial c_j = -\partial c_{3n+N} / \partial c_j$ for all $j \leq 3n + N - 1$. It follows that the determinant (46) equals to

$$\det \left(\frac{\partial(Q_1, \dots, Q_{3n}, P'_1, \dots, P'_{N-1})}{\partial(c_1, \dots, c_{3n+N-1})} + \begin{pmatrix} \frac{\partial Q_1}{\partial c_{3n+N}} \\ \vdots \\ \frac{\partial Q_{3n}}{\partial c_{3n+N}} \\ 0 \\ \vdots \\ 0 \end{pmatrix} \begin{pmatrix} \frac{\partial c_{3n+N}}{\partial c_1} & \dots & \frac{\partial c_{3n+N}}{\partial c_{3n+N-1}} \end{pmatrix} \right). \quad (48)$$

On the other hand, the chain rule says that for any function f we have

$$\frac{\partial f}{\partial c_i} + \frac{\partial f}{\partial c_{3n+N}} \frac{\partial c_{3n+N}}{\partial c_i} = \frac{\partial \bar{f}}{\partial c_i} \quad (49)$$

where \bar{f} is obtained from f by eliminating c_{3n+N} by using (47). It follows that the determinant (48) is simplified to

$$\det \left(\frac{\partial(\bar{Q}_1, \dots, \bar{Q}_{3n}, P'_1, \dots, P'_{N-1})}{\partial(c_1, \dots, c_{3n+N-1})} \right) \quad (50)$$

where \bar{Q}_i are obtained from Q_i by eliminating c_{3n+N} by using (47). For simplicity we let $Q_i = \bar{Q}_i$, regarding them now as functions in c_1, \dots, c_{3n+N-1} . Since P'_1, \dots, P'_{N-1} are unchanged, we can apply this reduction until we remove all P'_i and c_{3n+i} for $i \geq 1$. It follows that

$$\delta_{3,c}(t) = \det \left(\frac{\partial(Q_1, \dots, Q_{3n})}{\partial(c_1, \dots, c_{3n})} \right) \quad (51)$$

where $Q_i(t) = tc_i - c'_i$ are functions in c_1, \dots, c_{3n} . This completes the proof, since Equation (51) equals to the \mathbb{C}^3 -torsion polynomial given in Theorem 3.2. \square

Claim 2. Equation (2) holds for $n = 2$ and for all Ptolemy assignments c on \mathcal{T}_φ with ρ_c irreducible.

Proof. We label the faces of \mathcal{T}_φ as in Section 3.1: the faces of Σ are labeled with $\theta_1, \dots, \theta_{2n}$ and the new two faces created when we attach the i -th tetrahedron Δ_i is labeled by $\theta_{2n+2i-1}$ and θ_{2n+2i} for $1 \leq i \leq N$. Note that some faces have multiple labels. Then the face equations E_{2i-1} and E_{2i} for the top faces of Δ_i are written as

$$\begin{aligned} E_{2i-1} : \quad & c_{T(i)}\theta_{2n+2i-1} - c_{E_1(i)}\theta_{\alpha(i)} + c_{E_2(i)}\theta_{\beta(i)} = 0 \\ E_{2i} : \quad & c_{T(i)}\theta_{2n+2i} - c_{E_3(i)}\theta_{\alpha(i)} + c_{E_4(i)}\theta_{\beta(i)} = 0 \end{aligned} \quad (52)$$

where $\theta_{\alpha(i)}$ and $\theta_{\beta(i)}$ are the bottom faces of Δ_i and $c_{E_1(i)}, \dots, c_{E_4(i)}$ are the equatorial edges of Δ_i . Note that $\alpha(i), \beta(i) \leq 2n + 2i - 2$ and that $\{c_{T(1)}, \dots, c_{T(N)}\}$ is the edge set of \mathcal{T}_φ . Then, as we explained in Section 2.3, the 1-loop polynomial $\delta_{2,c}(t)$ is given by

$$\delta_{2,c}(t) = \left(\prod_{i=1}^N \frac{1}{c_{T(i)}} \right)^2 \det \left(\frac{\partial(F_1, \dots, F_{2n}, E_1, \dots, E_{2N})}{\partial(\theta_1, \dots, \theta_{2n+2N})} \right) \quad (53)$$

where $F_i = t\theta_i - \theta'_i$ for $1 \leq i \leq 2n$ where θ'_i is the super-Ptolemy variable on the top surface at the same position as θ_i . It follows that

$$\delta_{2,c}(t) = \det \left(\frac{\partial(F_1, \dots, F_{2n}, E'_1, \dots, E'_{2N})}{\partial(\theta_1, \dots, \theta_{2n+2N})} \right) = \det \left(\begin{array}{ccc|cc} t & & * & & \\ & \ddots & & & \\ * & & t & & * \\ \hline & & & 1 & 0 \\ & * & & * & 1 \end{array} \right). \quad (54)$$

where $E'_{2i-1} = E_{2i-1}/c_{T(i)}$ and $E'_{2i} = E_{2i}/c_{T(i)}$ for $1 \leq i \leq N$. Then the same reduction that we used in the proof of Claim 1 shows that

$$\delta_{2,c}(t) = \det \left(\frac{\partial(F_1, \dots, F_{2n})}{\partial(\theta_1, \dots, \theta_{2n})} \right) \quad (55)$$

where $F_i = t\theta_i - \theta'_i$ are now functions in $\theta_1, \dots, \theta_{2n}$. This completes the proof, since Equation (55) equals to the \mathbb{C}^2 -torsion polynomial given in Theorem 3.3. \square

We now discuss the second comment after the statement of Theorem 1.2. When M_φ is hyperbolic, the geometric $\mathrm{PSL}_2(\mathbb{C})$ -representation lifts to an $\mathrm{SL}_2(\mathbb{C})$ -representation (see [Cul86]) and every such lift ρ^{geom} is of the form $\rho_{c^{\mathrm{geom}}}$ for a Ptolemy assignment c^{geom} on \mathcal{T}_φ . The latter claim follows from the fact that the edges of \mathcal{T}_φ are ideal arcs in Σ , hence homotopically non-peripheral [DG12, HRST15]. Since every lift ρ^{geom} is clearly irreducible, we obtain

$$\delta_{n,c^{\mathrm{geom}}}(t) = \tau_{n,\rho^{\mathrm{geom}}}(t) \quad (56)$$

for $n = 2, 3$, as a special case of Theorem 1.2.

4. EXAMPLES

A census of oriented cusped hyperbolic manifolds `OrientableCuspedCensus` is given by `SnapPy` [CDGW], and of those, a list `CHW` of fibered ones is given by `flipper` [Bel21]. In this section we illustrate our theorems 3.2 and 3.3 with one of the first few manifolds from this list, namely for the fibered 3-manifold $M = \mathbf{m036}$, a one-cusped hyperbolic 3-manifold

with 4 tetrahedra and homology $H_1(M, \mathbb{Z}) = \mathbb{Z} + \mathbb{Z}/3\mathbb{Z}$, hence with two obstruction classes, a trivial one and a non-trivial one, and four boundary obstruction classes.

4.1. **The layered triangulation of m036.** The manifold $M = M_\varphi$ is fibered where its fiber $\Sigma = \Sigma_{2,1}$ is a once-punctured surface of genus 2 and its pseudo-Anosov monodromy is $\varphi = \text{aaabcd}$, where a, b, c, d are the positive Dehn twists on Σ shown in Figure 4.

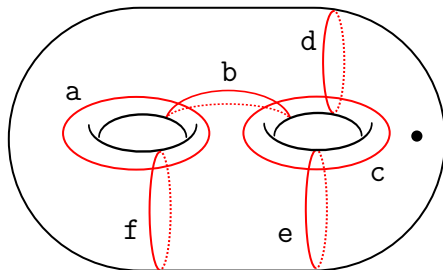


FIGURE 4. Dehn twists on $\Sigma_{2,1}$.

Among other things, `flipper` describes a triangulation of Σ , the monodromy φ and the layered triangulation. To begin with, the triangulated surface Σ is described by its list of 6 triangles ($\sim 8, \sim 1, \sim 4$), \dots , $(4, 5, 6)$, each encoded by a triple of edges taken counterclockwise. Note that Σ has 9 oriented edges $0, \dots, 8$ (where $\sim e$ denotes the orientation-reversed edge e).

```
1 sage: import snappy, flipper
2 sage: M = snappy.Manifold('m036')
3 sage: phi = flipper.monodromy_from_bundle(M)
4 sage: S = phi.source_triangulation; S
5 [(~8, ~1, ~4), (~7, ~3, 2), (~6, ~2, 1), (~5, 0, 3), (~0, 7, 8), (4, 5, 6)]
```

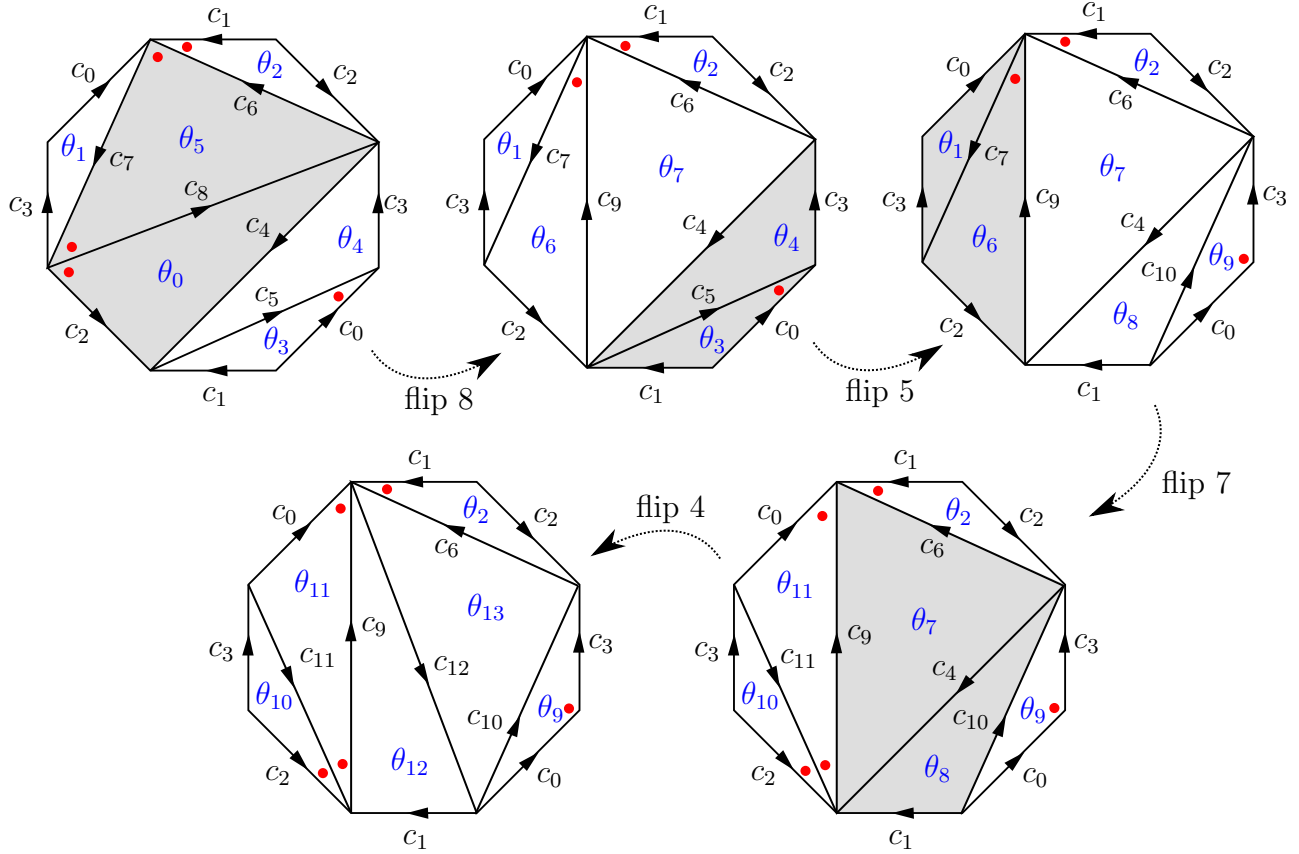
The monodromy φ is given by a product of moves that consist of combinatorial surface automorphisms and flips

```
1 sage: phi.sequence
2 [Isometry [1, 2, 3, 4, 5, 6, 7, 8, ~0], Flip 8, Flip 5, Flip 7, Flip 4]
```

Each flip adds a tetrahedron to the layered triangulation. Explicitly, the sequence of triangulations of Σ under these moves is given by

```
1 sage: for flip in phi.sequence[1:]:
2     ....:     print(flip.target_triangulation)
3     ....:
4 [(~8, 2, ~4), (~7, ~0, ~3), (~6, ~2, 1), (~5, ~1, 0), (3, 4, 5), (6, 7, 8)]
5 [(~8, ~4, 6), (~7, ~0, ~3), (~6, ~2, 1), (~5, ~1, 0), (2, 8, 7), (3, 4, 5)]
6 [(~8, ~4, 6), (~7, ~0, ~3), (~6, ~2, 1), (~5, 0, 3), (~1, 5, 4), (2, 8, 7)]
7 [(~8, ~4, 6), (~7, ~3, 2), (~6, ~2, 1), (~5, 0, 3), (~1, 5, 4), (~0, 7, 8)]
```

Starting with the triangulation of Σ after the combinatorial surface automorphism, the sequence of 4 flips is shown in Figure 5. Note that `flipper` reuses labels for edges; for instance, the first flip make the edge 8 disappear and create a new edge, which is also labeled with 8. However, to avoid confusion we will give new labels for new edges.


 FIGURE 5. Four flips for $m036$.

4.2. \mathbb{C}^3 -torsion polynomial. In this section we compute the \mathbb{C}^3 -torsion polynomial. As shown in Figure 5, the initial surface has nine Ptolemy variables c_0, \dots, c_8 . Attaching four tetrahedra to the surface, we obtain four additional variables c_9, \dots, c_{12} with four Ptolemy equations:

$$\begin{aligned}
 P_1 : \quad c_9 c_8 - c_2 c_6 - c_4 c_7 &= 0 \\
 P_2 : \quad c_{10} c_5 + c_1 c_3 + c_0 c_4 &= 0 \\
 P_3 : \quad c_{11} c_7 + c_2 c_0 - c_3 c_9 &= 0 \\
 P_4 : \quad c_{12} c_4 + c_1 c_6 - c_9 c_{10} &= 0
 \end{aligned} \tag{57}$$

Solving these equations determines the additional variables c_9, \dots, c_{12} as

$$\begin{aligned}
 (c_9, \dots, c_{12}) = & \left(\frac{c_2 c_6 + c_4 c_7}{c_8}, -\frac{c_1 c_3 + c_0 c_4}{c_5}, \frac{c_2 c_3 c_6 + c_3 c_4 c_7 - c_0 c_2 c_8}{c_7 c_8}, \right. \\
 & \left. -\frac{c_0 c_4 (c_2 c_6 + c_4 c_7) + c_1 (c_2 c_3 c_6 + c_3 c_4 c_7 + c_5 c_6 c_8)}{c_4 c_5 c_8} \right).
 \end{aligned} \tag{58}$$

We isotope the initial surface as in Figure 6 so that it can be identified with the terminal surface given in Figure 5 in an obvious way. As in Section 3, we denote by (c'_0, \dots, c'_8) the Ptolemy variables on the terminal surface

$$(c'_0, c'_1, c'_2, c'_3, c'_4, c'_5, c'_6, c'_7, c'_8) = (c_1, c_2, c_3, c_{12}, c_{10}, c_6, c_{11}, c_9, -c_0). \tag{59}$$

so that solving $c'_i = c_i$ for $0 \leq i \leq 8$ gives a Ptolemy assignment on \mathcal{T}_φ . Precisely, the solutions to $c'_i = c_i$ for $0 \leq i \leq 8$ are

$$(c_0, c_1, c_2, c_3, c_4, c_5, c_6, c_7, c_8) = c(1, 1, 1, 1, \beta, 1 - \beta, 1 - \beta, \beta - 2, -1), \quad c \in \mathbb{C}^* \quad (60)$$

where β is a solution to

$$\beta^2 - 2\beta - 1 = 0. \quad (61)$$

Applying Theorem 3.2, we obtain

$$\tau_{3,\rho_c}(t) = \det \left(tI - \frac{\partial c'_i}{\partial c_j} \right) = -1 + 4t + 2t^3 + t^4 + t^5 + 2t^6 + 4t^8 + t^9.$$

Note that this polynomial does not come from a lift of the geometric representation, as such a lift always has a peripheral curve whose image under the lift has trace -2 .

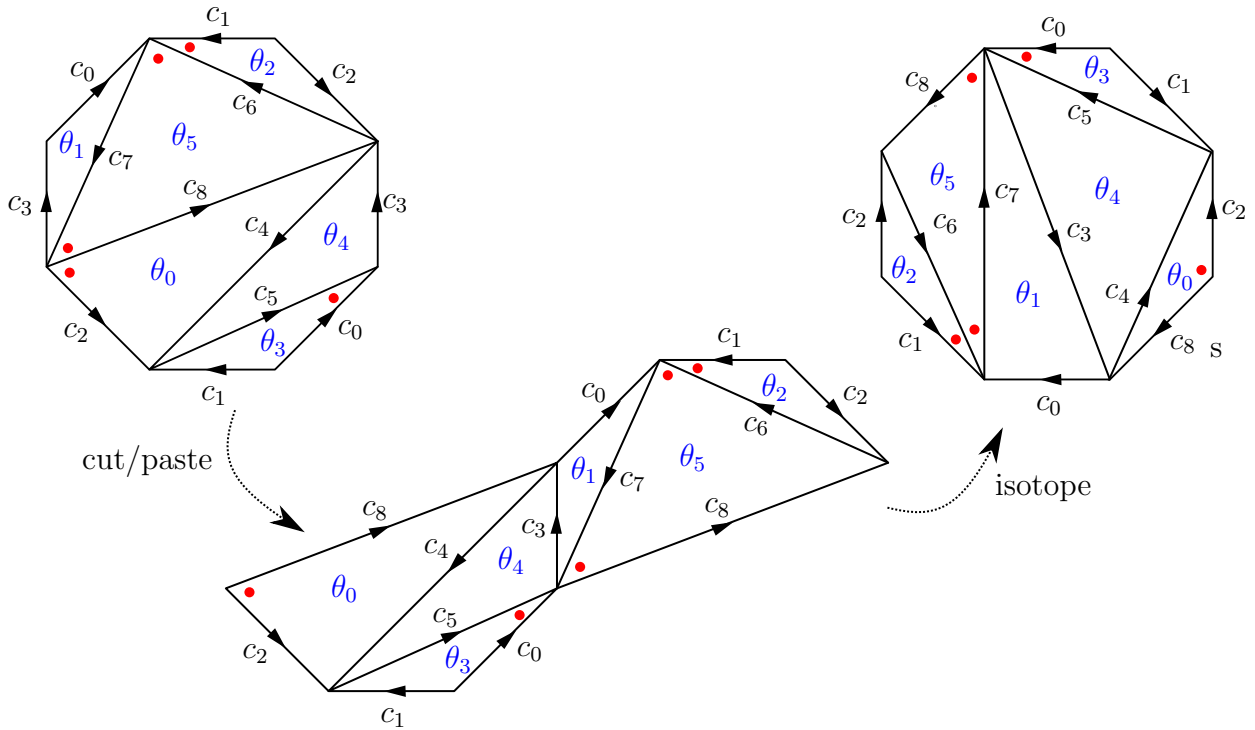


FIGURE 6. Modifying the initial surface.

To cover a lift of the geometric representation, we need the sign-deformation of the equations as in Section 2.4. Recall that this is done by assigning a sign to every short edge of (the truncated triangulation of) \mathcal{T}_φ . As shown in Figure 5, we assign -1 if a short edge is red-dotted, and $+1$, otherwise. Note that each surface in Figure 5 has an odd number of red dots, and this implies that a curve that winds the puncture of each surface maps to an $SL_2(\mathbb{C})$ -matrix of trace -2 (we refer to [Yoo] for details). According to this sign-assignment,

the Ptolemy equations (57) change to

$$\begin{aligned}
P_1 : \quad c_9c_8 + c_2c_6 - c_4c_7 &= 0 \\
P_2 : \quad c_{10}c_5 + c_1c_3 - c_0c_4 &= 0 \\
P_3 : \quad c_{11}c_7 - c_2c_0 - c_3c_9 &= 0 \\
P_4 : \quad c_{12}c_4 + c_1c_6 - c_9c_{10} &= 0
\end{aligned} \tag{62}$$

with

$$(c_9, \dots, c_{12}) = \left(\frac{-c_2c_6 + c_4c_7}{c_8}, \frac{-c_1c_3 + c_0c_4}{c_5}, \frac{-c_2c_3c_6 + c_3c_4c_7 + c_0c_2c_8}{c_7c_8}, \right. \\
\left. \frac{c_0c_4(-c_2c_6 + c_4c_7) + c_1(c_2c_3c_6 - c_3c_4c_7 - c_5c_6c_8)}{c_4c_5c_8} \right). \tag{63}$$

Then solving $c'_i = c_i$ for $0 \leq i \leq 8$ we obtain

$$(c_0, c_1, c_2, c_3, c_4, c_5, c_6, c_7, c_8) = c(1, 1, 1, 1, \alpha, -\alpha - \alpha^2, -\alpha - \alpha^2, -\alpha, -1), \quad c \in \mathbb{C}^* \tag{64}$$

where α is a solution to

$$\alpha^3 + \alpha^2 + \alpha - 1 = 0, \quad \alpha^{\text{geom}} \approx -0.77184 + 1.11514 \cdot i \tag{65}$$

with α^{geom} corresponding to (a lift of) the geometric representation. Applying Theorem 3.2, we obtain

$$\begin{aligned}
\tau_{3,\rho c}(t) = & -1 - (2\alpha^2 + 4\alpha + 2)t - (4\alpha^2 + 6\alpha + 6)t^2 - (6\alpha^2 + 4\alpha + 8)t^3 + (2\alpha^2 - 4\alpha - 3)t^4 \\
& + (-2\alpha^2 + 4\alpha + 3)t^5 + (6\alpha^2 + 4\alpha + 8)t^6 + (4\alpha^2 + 6\alpha + 6)t^7 + (2\alpha^2 + 4\alpha + 2)t^8 + t^9.
\end{aligned}$$

Using the numerical value of α^{geom} from (65), this matches (after multiplication with -1 , and after renaming the ‘t’ variable by ‘a’) with the \mathbb{C}^2 -torsion polynomial of m036 computed in SnapPy

```

1 sage: snappy.Manifold('m036').hyperbolic_SLN_torsion(3, bits_prec=50)
2 -1.00000000000003*a^9 + (2.3829757679074 - 1.0177035576648*I)*a^8 +
  (1.2222625231179 + 0.19487790074776*I)*a^7 + (-1.0258287470449 +
  5.8680293913261*I)*a^6 + (-1.2082197171469 - 7.9034365066556*I)*a^5 +
  (1.2082197171534 + 7.9034365066503*I)*a^4 + (1.0258287470263 -
  5.8680293913033*I)*a^3 + (-1.2222625230950 - 0.19487790079827*I)*a^2 +
  (-2.3829757679132 + 1.0177035577685*I)*a + 0.99999999993775

```

Before we move on to discuss the \mathbb{C}^2 -torsion polynomial, note that M has 4 boundary obstruction classes and we presented the Ptolemy and face equations for only two of them. One can analyze the remaining two similarly, but we will not give the details here.

4.3. \mathbb{C}^2 -torsion polynomial. We finally discuss the \mathbb{C}^2 -torsion polynomial. As shown in Figure 5, the initial surface has six super-Ptolemy variables $\theta_0, \dots, \theta_5$. Attaching four tetrahedra to the surface, we obtain eight additional variables $\theta_6, \dots, \theta_{13}$ with eight additional

face equations:

$$\begin{aligned}
E_1 : & \quad c_2\theta_0 + c_9\theta_7 + c_7\theta_5 & = 0 \\
E_2 : & \quad -c_4\theta_0 + c_6\theta_5 - c_9\theta_6 & = 0 \\
E_3 : & \quad -c_1\theta_3 + c_{10}\theta_9 + c_4\theta_4 & = 0 \\
E_4 : & \quad c_0\theta_3 + c_3\theta_4 - c_{10}\theta_8 & = 0 \\
E_5 : & \quad c_2\theta_6 - c_{11}\theta_{11} - c_3\theta_1 & = 0 \\
E_6 : & \quad c_9\theta_6 - c_0\theta_4 + c_{11}\theta_{10} & = 0 \\
E_7 : & \quad -c_1\theta_8 - c_{12}\theta_{13} - c_9\theta_7 & = 0 \\
E_8 : & \quad c_{10}\theta_8 + c_6\theta_7 + c_{12}\theta_{12} & = 0
\end{aligned} \tag{66}$$

Solving these equations determines the additional variables $\theta_6, \dots, \theta_{13}$ as

$$(\theta_6, \dots, \theta_{13}) = \left(\frac{c_6\theta_5 - c_4\theta_0}{c_9}, -\frac{c_7\theta_5 + c_2\theta_0}{c_9}, \frac{c_3\theta_4 + c_0\theta_3}{c_{10}}, \frac{-c_4\theta_4 + c_1\theta_3}{c_{10}}, \frac{c_0\theta_1 - c_6\theta_5 + c_4\theta_0}{c_{11}}, \right. \\
\left. -\frac{c_3c_9\theta_1 - c_2c_6\theta_5 + c_2c_4\theta_0}{c_{11}c_9}, \frac{c_6c_7\theta_5 + c_2c_6\theta_0 - c_3c_9\theta_4 - c_0c_9\theta_3}{c_{12}c_9}, \frac{c_{10}c_7\theta_5 + c_{10}c_2\theta_0 - c_1c_3\theta_4 - c_0c_1\theta_3}{c_{10}c_{12}} \right).$$

If we denote by $(\theta'_0, \dots, \theta'_5)$ the super-Ptolemy variables on the terminal surface

$$(\theta'_0, \theta'_1, \theta'_2, \theta'_3, \theta'_4, \theta'_5) = (\theta_9, \theta_{12}, \theta_{10}, \theta_2, \theta_{13}, \theta_{11}) \tag{67}$$

so that solving $\theta'_i = \theta_i$ for $0 \leq i \leq 5$ gives a super-Ptolemy assignment on \mathcal{T}_φ , then Theorem 3.3 with a Ptolemy assignment given in (60) gives

$$\tau_{2,\rho_c}(t) = \det \left(tI - \frac{\partial \theta'_i}{\partial \theta_j} \right) = 1 - 2t + t^2 + t^4 - 2t^5 + t^6.$$

If we use the sign-deformation given in Section 4.2, the face equations (66) change to

$$\begin{aligned}
E_1 : & \quad -c_2\theta_0 + c_9\theta_7 - c_7\theta_5 & = 0 \\
E_2 : & \quad +c_4\theta_0 + c_6\theta_5 - c_9\theta_6 & = 0 \\
E_3 : & \quad -c_1\theta_3 + c_{10}\theta_9 - c_4\theta_4 & = 0 \\
E_4 : & \quad c_0\theta_3 + c_3\theta_4 - c_{10}\theta_8 & = 0 \\
E_5 : & \quad c_2\theta_6 - c_{11}\theta_{11} + c_3\theta_1 & = 0 \\
E_6 : & \quad -c_9\theta_6 + c_0\theta_4 + c_{11}\theta_{10} & = 0 \\
E_7 : & \quad -c_1\theta_8 - c_{12}\theta_{13} - c_9\theta_7 & = 0 \\
E_8 : & \quad c_{10}\theta_8 + c_6\theta_7 + c_{12}\theta_{12} & = 0
\end{aligned} \tag{68}$$

which give

$$(\theta_6, \dots, \theta_{13}) = \left(\frac{c_6\theta_5 + c_4\theta_0}{c_9}, \frac{c_7\theta_5 + c_2\theta_0}{c_9}, \frac{c_3\theta_4 + c_0\theta_3}{c_{10}}, \frac{c_4\theta_4 + c_1\theta_3}{c_{10}}, \frac{-c_0\theta_1 + c_6\theta_5 + c_4\theta_0}{c_{11}}, \right. \\ \left. \frac{c_3c_9\theta_1 + c_2c_6\theta_5 + c_2c_4\theta_0}{c_{11}c_9}, \frac{-c_6c_7\theta_5 + c_2c_6\theta_0 + c_3c_9\theta_4 + c_0c_9\theta_3}{c_{12}c_9}, \right. \\ \left. - \frac{c_{10}c_7\theta_5 + c_{10}c_2\theta_0 + c_1c_3\theta_4 + c_0c_1\theta_3}{c_{10}c_{12}} \right).$$

Applying Theorem 3.3 with a Ptolemy assignment given in (64), we obtain

$$\tau_{2,\rho_c}(t) = 1 + (2\alpha^2 + 2\alpha + 2)t + (\alpha^2 + 2\alpha + 4)t^2 + (2\alpha^2 + 4\alpha + 2)t^3 + (\alpha^2 + 2\alpha + 4)t^4 \\ + (2\alpha^2 + 2\alpha + 2)t^5 + t^6$$

where α is a solution to Equation (65). Using the numerical value of α^{geom} from (65), this matches (after renaming the ‘t’ variable by ‘a’) with the \mathbb{C}^2 -torsion polynomial of `m036` computed in `SnapPy`

```
1 sage: snappy.Manifold('m036').hyperbolic_SLN_torsion(2, bits_prec=50)
2 a^6 + (-0.83928675521416 - 1.2125814584144*I)*a^5 + (1.8085121160469 +
  0.50885177883279*I)*a^4 + (-2.3829757679062 + 1.0177035576654*I)*a^3 +
  (1.8085121160468 + 0.50885177883267*I)*a^2 + (-0.83928675521427 -
  1.2125814584143*I)*a + 1.00000000000002
```

5. EVIDENCE THE CONJECTURE HOLDS FOR NONFIBERED MANIFOLDS

In this section, we discuss computations showing that Conjecture 1.1 holds for at least one triangulation of 6,672 distinct nonfibered hyperbolic 3-manifolds, of which 14.4% are exteriors of knots in S^3 . Combined with Theorem 1.2, this gives compelling evidence for Conjecture 1.1. For all the computations discussed here, both the source code and the raw data can be found at [DGY].

5.1. Sample manifolds. Our initial list of manifolds was drawn from two sources. The first is Burton’s census of cusped orientable hyperbolic 3-manifolds that can be triangulated with at most 9 ideal tetrahedra [Bur], where we considered the 59,068 such manifolds where $b_1(M) = 1$. (This census also contains 2,843 manifolds with $b_1(M) > 1$.) The second source was 1,692 hyperbolic knots in S^3 , each with less than 14 crossings, whose exteriors had an ideal triangulation with at most 16 tetrahedra. These overlap in 189 manifolds, so full sample size is 60,571 distinct manifolds. These manifolds were chosen because each one has a triangulation where Goerner found exact representations for all possible Ptolemy assignments [Goe]. Specifically, for each such assignment he specifies a number field K as $\mathbb{Q}[x]/(f(x))$, where $f(x) \in \mathbb{Z}[x]$ is irreducible, and the assignment $c: \mathcal{T}^1 \rightarrow K^*$ by a polynomial in x for each edge.

5.2. Thurston norm and fibering. All these manifolds have $b_1(M) = 1$, and for such we define $x(M) \in \mathbb{Z}_{\geq 0}$ to be the Thurston norm of a generator of $H^1(M; \mathbb{Z})$. For all our sample, we were able to calculate $x(M)$ using the following technique based on ideas of Lackenby [Lac00]. For each manifold, triangulations were generated randomly until one was found with a co-orientable taut structure whose horizontal branched surface carried a non-empty

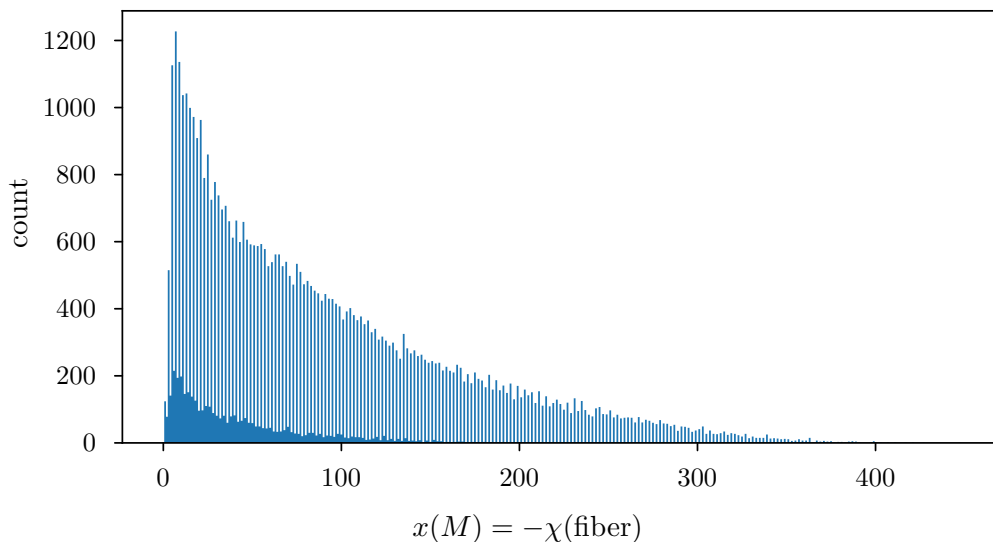


FIGURE 7. A histogram of the Thurston norm $x(M)$ for the 53,896 fibered manifolds in our sample, with mean 86.1, median 65, and max 447. Here, each bar corresponds to the number of manifolds with a single value of $x(M)$, e.g. the tallest bar represents the 1,227 manifolds where $x(M) = 7$ (for 89.8% of these, the fiber is genus 4 with one puncture). In this sample, it is much more common for $x(M)$ to be odd (93.0%) than even (7.0%), and so the bars alternate between tall and short. Compare with Figure 8.

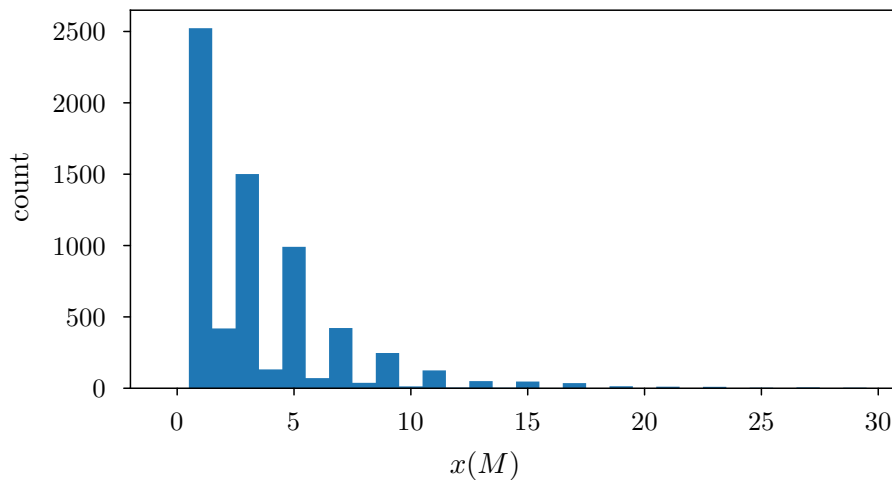


FIGURE 8. A histogram of the Thurston norm $x(M)$ for the 6,675 nonfibered manifolds in our sample, with mean 3.6, median 2, and max 29. Compare Figure 7, where the mean $x(M)$ is 23.9 times larger. Despite this, the fibered and nonfibered manifolds in the sample have very similar volumes and numbers of tetrahedra; see also Figure 9.

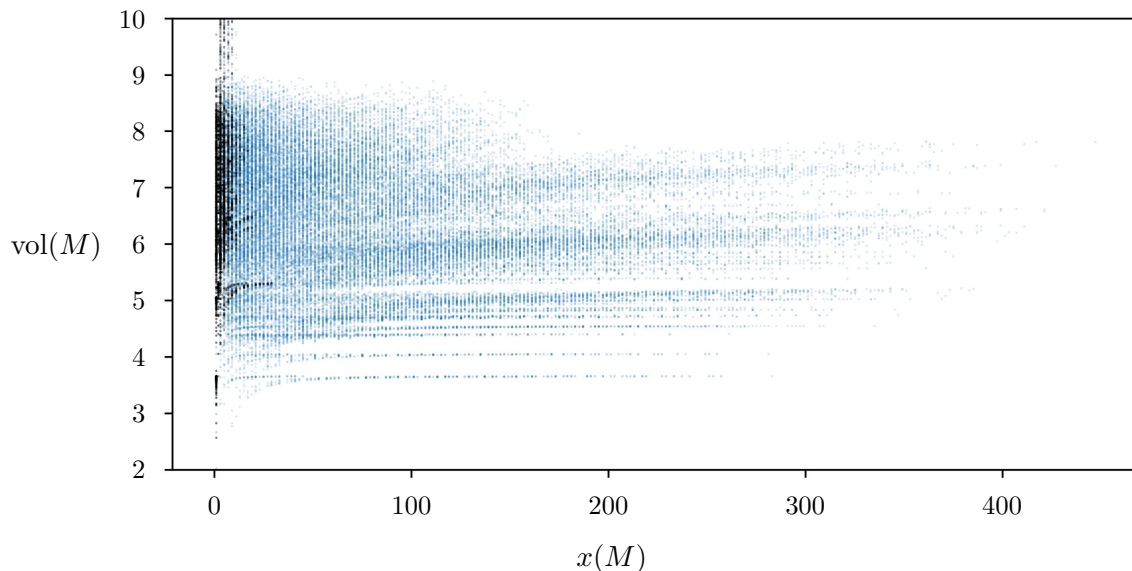


FIGURE 9. A scatter plot of the Thurston norm $x(M)$ as compared to the hyperbolic volume $\text{vol}(M)$ for the 60,571 manifolds in the sample. Here, fibered manifolds are shown in blue and nonfibered manifolds in black. Some 1,222 manifolds with $\text{vol}(M) > 10$ are not shown (2% of the sample), all of which have $x(M) \leq 11$ and are exteriors of knots in S^3 . Some of the structure, e.g. the large number of fibered manifolds with volume roughly 3.66, comes from hyperbolic Dehn surgery.

surface (not necessarily with full support). Taking said surface F to be connected, its class generates $H_2(M, \partial M; \mathbb{Z})$ and, by [Lac00], it realizes the Thurston norm of $[F]$.

We also determined which of these manifolds fiber over the circle: 53,896 (89.0%) do and 6,675 (11.0%) do not. (For 6,276 (10.4%) of these, this was previously done in [But05] or [DFJ12].) First, we showed that 53,896 of these manifolds fiber over the circle as follows. In all but six cases, we were able to find a co-orientable taut structure whose horizontal branched surface carries a surface with *full support*. Equivalently, we found a taut layered ideal triangulation for the manifold as in Section 3. The other six fibered manifolds, which were the census manifolds $o9_{33772}$, $o9_{39015}$, $o9_{39073}$, $o9_{40271}$, $o9_{41509}$, and $o9_{43580}$, were handled by ad hoc methods that are detailed in [DGY]. The remaining 6,675 manifolds were shown to be nonfibered using (a) that the ordinary Alexander polynomial was not monic (6,463 manifolds), or (b) that some (exactly computed) twisted Alexander polynomial was not monic (212 manifolds).

Of the 6,675 distinct nonfibered manifolds, exactly 964 (14.5%) of them are exteriors of knots in the 3-sphere by [Dun20].

5.3. Checking that 1-loop equals torsion. For each of the 6,675 nonfibered manifolds, we tried to check Conjecture 1.1 for the preferred triangulation \mathcal{T} and all Ptolemy assignments which are part of 0-dimensional components of the reduced Ptolemy variety $P_2(\mathcal{T})_{\text{red}} := P_2(\mathcal{T})/(\mathbb{C}^*)^b$. (Any assignment associated to the hyperbolic structure is on

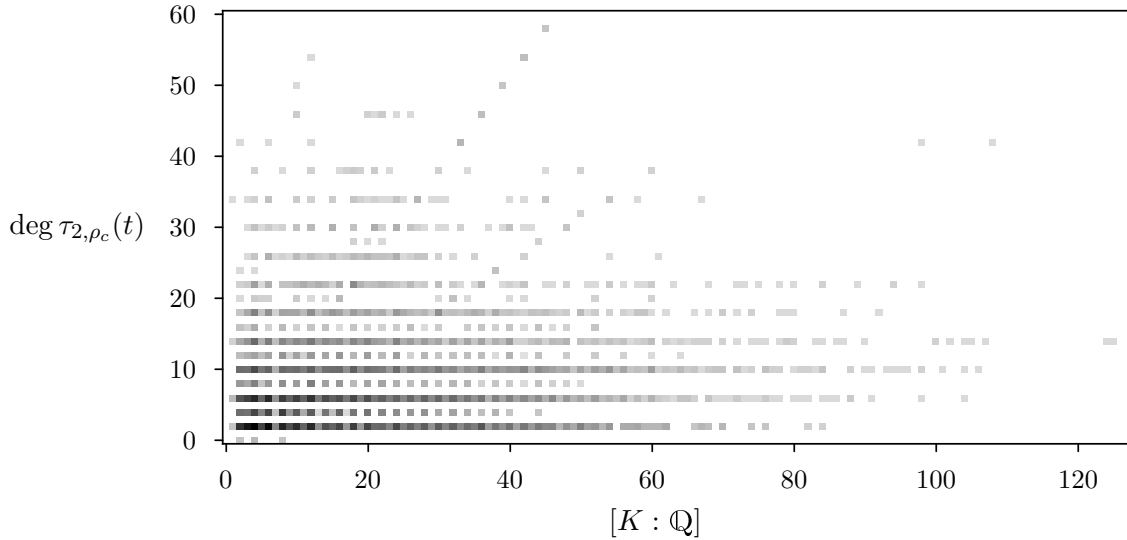


FIGURE 10. A density plot exploring the 29,948 Ptolemy assignments $c: \mathcal{T}^1 \rightarrow K^*$ of 6,672 nonfibered hyperbolic 3-manifolds and their \mathbb{C}^2 -torsion polynomials where we checked Conjecture 1.1. Here, K is viewed as an abstract number field so that c describes a $\text{Gal}(\overline{\mathbb{Q}}/\mathbb{Q})$ -orbit of such assignments; these encode more than 500,000 distinct concrete Ptolemy assignments $c: \mathcal{T}^1 \rightarrow \mathbb{C}^*$. Note here that $\deg \tau_{2, \rho_c}(t)$ is always even because of its symmetry under $t \mapsto t^{-1}$.

such a component, and only 162 of these triangulations have any components of positive dimension.) We succeeded for all but three manifolds where the computation did not finish due to the extreme complexity (the exceptions were $o9_{18365}$, $o9_{20926}$, and $o9_{31289}$). Recall that $P_2(\mathcal{T})_{\text{red}}$ is defined over \mathbb{Q} , and hence each 0-dimensional irreducible component over \mathbb{C} (i.e. each isolated point) necessarily has coordinates in $\overline{\mathbb{Q}}$. The group $\text{Gal}(\overline{\mathbb{Q}}/\mathbb{Q})$ acts on such points, with the orbits being the 0-dimensional \mathbb{Q} -irreducible components. In particular, each such orbit of size d has an associated number field K of degree d with a Ptolemy assignment $c: \mathcal{T}^1 \rightarrow K^*$ which gives all points on this orbit by considering the d distinct embeddings $K \hookrightarrow \mathbb{C}$. As mentioned, the complete list of such Ptolemy assignments for these manifolds was computed by Goerner [Goe].

For each manifold M , and boundary obstruction class σ , and sign-deformed Ptolemy solution $c: \mathcal{T}^1 \rightarrow K^*$ on such a component, we checked Conjecture 1.1 by exact arithmetic in the number field K . There was a mean of 4.5 such (σ, c) pairs per manifold, where $[K : \mathbb{Q}]$ had median 15, mean 18.8, and a maximum of 125. (There are four possible $\sigma \in H^1(\partial M; \mathbb{Z}/2\mathbb{Z})$, two of which are compatible with Ptolemy assignments associated to the hyperbolic structure. Each of the triangulations used supports the hyperbolic structure, so there were always at least two such pairs (σ, c) .) The resulting \mathbb{C}^2 -torsion polynomials had median degree 6, mean degree 7.0, and maximum degree 58, see Figure 10. For the \mathbb{C}^3 -torsion polynomial, the degree had median 9, mean 10.4, and maximum 87.

Remark 5.1. To validate our code for checking Conjecture 1.1, we also ran it on 18,588 of the *fibred* manifolds in our sample. The number of pairs (σ, c) was similar at 4.1, but $[K : \mathbb{Q}]$ was larger, with median 26, mean 28.9, and max 140.

5.4. Lower bounds on the Thurston norm. For a knot K in S^3 with exterior $E_K = S^3 \setminus \nu(K)$, set $x(K) = x(E_K)$; equivalently

$$x(K) = -\chi(\text{minimal Seifert surface}) = 2 \cdot \text{genus}(K) - 1.$$

As mentioned in Section 1, if K is a hyperbolic knot in S^3 then for the \mathbb{C}^2 -torsion one has:

$$x(K) \geq \frac{1}{2} \deg \tau_{2, \rho^{\text{geom}}}(t)$$

where ρ^{geom} is any lift of the holonomy representation to $\text{SL}_2(\mathbb{C})$. This inequality is an equality for all such knots with at most 15 crossings, of which there are more than 300,000, leading to Conjecture 1.7 of [DFJ12]:

Conjecture 5.2 (Dunfield-Friedl-Jackson). If K is a hyperbolic knot in S^3 , then $x(K) = \frac{1}{2} \deg \tau_{2, \rho^{\text{geom}}}(t)$. Moreover, its exterior fibers over the circle if and only if $\tau_{2, \rho^{\text{geom}}}(t)$ is monic.

While there is an analogous bound on the Thurston norm from the degree of the \mathbb{C}^3 -torsion polynomial, this it is not always sharp [DFJ12, Section 6.6].

It is natural to ask what happens for more general M . First, the lower bound $x(M) \geq \frac{1}{2} \deg \tau_{2, \rho^{\text{geom}}}(t)$ holds for any cusped hyperbolic 3-manifold with $b_1(M) = 1$, and $\tau_{2, \rho^{\text{geom}}}$ is monic whenever M fibers over the circle; see e.g. Theorem 1.5 of [DFJ12], where the assumption on the $\mathbb{Z}/2\mathbb{Z}$ -homology of M is unnecessary. However, a new wrinkle is that $\tau_{2, \rho^{\text{geom}}}(t)$ can change dramatically depending on which lift ρ^{geom} is chosen; this was noted in [DFJ12, Remark 4.7] and also illustrated by Examples 5.3 and 5.4 below.

Recall that if a representation $\bar{\rho}: \pi_1(M) \rightarrow \text{PSL}_2(\mathbb{C})$ lifts to $\rho: \pi_1(M) \rightarrow \text{SL}_2(\mathbb{C})$ there are $H^1(M; \mathbb{Z}/2\mathbb{Z})$ distinct lifts, where the latter is viewed as homomorphisms from $\pi_1(M)$ to the center $\{\pm I\}$ of $\text{SL}_2(\mathbb{C})$. When $H^1(M; \mathbb{Z}/2\mathbb{Z}) \cong \mathbb{Z}/2\mathbb{Z}$, for example for the exterior of a knot in S^3 , then the two lifts ρ and ψ of the holonomy representation satisfy $\tau_{2, \rho}(t) = \tau_{2, \psi}(-t)$ by [DFJ12, Remark 4.6] and so contain equivalent information. To understand the general situation, we need to study the map $H_1(\partial M; \mathbb{Z}) \rightarrow H_1(M; \mathbb{Z})$ in minute detail.

5.5. Labeling the boundary obstruction classes. Let M be an orientable 3-manifold where ∂M is a torus with no restriction on $b_1(M)$. For a field \mathbb{F} , an \mathbb{F} -*longitude* is a *primitive* element of $H_1(\partial M; \mathbb{Z})$ that becomes 0 in $H_1(M; \mathbb{F})$; these always exist as the kernel of $i_*: H_1(\partial M; \mathbb{F}) \rightarrow H_1(M; \mathbb{F})$ is 1-dimensional. A \mathbb{Q} -longitude is the same as either of the generators of the kernel of

$$i_*: H_1(\partial M; \mathbb{Z}) \rightarrow H_1(M; \mathbb{Z})/\text{torsion} \tag{69}$$

A \mathbb{Q} -longitude need not be a $\mathbb{Z}/2\mathbb{Z}$ -longitude, and in this situation we say M is $\mathbb{Z}/2\mathbb{Z}$ -*askew*; see Figure 11 for the example of the twisted I -bundle over the Klein bottle. If instead each \mathbb{Q} -longitude is a $\mathbb{Z}/2\mathbb{Z}$ -longitude, we say that M is $\mathbb{Z}/2\mathbb{Z}$ -*aligned*. For example, the exterior of any knot in S^3 is $\mathbb{Z}/2\mathbb{Z}$ -aligned. Note that M is $\mathbb{Z}/2\mathbb{Z}$ -askew if and only if the composition $H^1(M; \mathbb{Z}) \rightarrow H^1(\partial M; \mathbb{Z}) \rightarrow H^1(\partial M; \mathbb{Z}/2\mathbb{Z})$ is 0. In our sample of nonfibred manifolds,

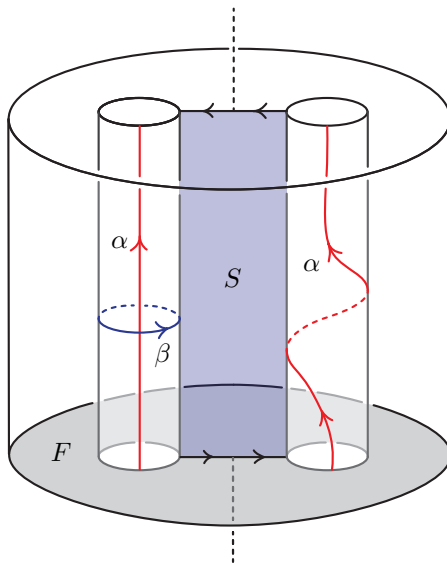


FIGURE 11. A simple 3-manifold that is $\mathbb{Z}/2\mathbb{Z}$ -askew. Let F be an annulus and consider $F \times [0, 1]$ as shown above where each copy of F includes the rest of the plane it lies in plus a point at infinity. Let M be the mapping torus of the self-homeomorphism of F that interchanges the two boundary components and looks like rotation by π about the indicated vertical axis. Note that any copy of F generates $H_2(M; \mathbb{Z}) \cong H^1(M; \mathbb{Z}) \cong \mathbb{Z}$. The vertical strip shown becomes a Möbius band S in M with $H_2(M; \mathbb{Z}/2\mathbb{Z}) \cong H^1(M; \mathbb{Z}/2\mathbb{Z}) \cong (\mathbb{Z}/2\mathbb{Z})^2$ generated by $[F]$ and $[S]$. Here, the curve β is a \mathbb{Q} -longitude as $2\beta = \partial F$, but not a $\mathbb{Z}/2\mathbb{Z}$ -longitude as it meets S once.

92.3% are $\mathbb{Z}/2\mathbb{Z}$ -aligned and 7.7% are $\mathbb{Z}/2\mathbb{Z}$ -askew (for the fibered manifolds the breakdown is 93.8% and 6.2%).

We define a *homologically reasonable framing* to be a generating set (α, β) for $H_1(\partial M; \mathbb{Z})$ where β is a \mathbb{Q} -longitude and α is *not* a $\mathbb{Z}/2\mathbb{Z}$ -longitude. Here, α will generate the image of i_* in (69), as well as image of $i_*: H_1(\partial M; \mathbb{Z}/2\mathbb{Z}) \rightarrow H_1(M; \mathbb{Z}/2\mathbb{Z})$. When M is the exterior of a knot in S^3 , any standard (meridian, longitude) basis is homologically reasonable. See Figure 11 for such a basis when M is $\mathbb{Z}/2\mathbb{Z}$ -askew. Note β is unique up to sign, and the possible α are $\alpha' = \pm\alpha + n\beta$ where $n \in 2\mathbb{Z}$ if M is $\mathbb{Z}/2\mathbb{Z}$ -askew and $n \in \mathbb{Z}$ otherwise.

If (α, β) is a homologically reasonable framing, consider the map $H^1(\partial M; \mathbb{Z}/2\mathbb{Z}) \rightarrow (\mathbb{Z}/2\mathbb{Z})^2$ talking ϕ to $(\phi(\alpha), \phi(\beta))$. We label the four elements of $H^1(\partial M; \mathbb{Z}/2\mathbb{Z})$ lexicographically as

$$\sigma_0, \sigma_1, \sigma_2, \sigma_3 = [(0, 0), (0, 1), (1, 0), (1, 1)].$$

Here, the image of $i^*: H^1(M; \mathbb{Z}/2\mathbb{Z}) \rightarrow H^1(\partial M; \mathbb{Z}/2\mathbb{Z})$ is $\{\sigma_0, \sigma_2\}$ when M is $\mathbb{Z}/2\mathbb{Z}$ -aligned and $\{\sigma_0, \sigma_3\}$ when M is $\mathbb{Z}/2\mathbb{Z}$ -askew.

When M is $\mathbb{Z}/2\mathbb{Z}$ -aligned, this labeling is not canonical: a different framing can interchange σ_1 and σ_3 , specifically $(\alpha + \beta, \beta)$. However, when M is $\mathbb{Z}/2\mathbb{Z}$ -askew, labeling is

independent of the homologically reasonable framing. (A coordinate-free way to see this is that σ_0 is the identity element, σ_3 is the nonzero element in the image of $H^1(M; \mathbb{Z}/2\mathbb{Z})$, and σ_2 is the nonzero element that vanishes on the \mathbb{Q} -longitude.)

Now suppose $b_1(M) = 1$ and let ϵ_∞ be the unique nonzero element in the image of $H^1(M; \mathbb{Z}) \rightarrow H^1(M; \mathbb{Z}/2\mathbb{Z})$. If $\rho: \pi_1(M) \rightarrow \mathrm{SL}_2(\mathbb{C})$, then $\tau_\rho(t) = \tau_{\epsilon_\infty \cdot \rho}(-t)$ as in [DFJ12, Remark 4.6]. When M is $\mathbb{Z}/2\mathbb{Z}$ -aligned, the restriction of ϵ_∞ to ∂M is σ_2 . Thus if c is a Ptolemy solution for the boundary obstruction class σ_i , there is a corresponding c' with boundary obstruction class $\sigma_{i+2 \pmod{4}}$ so that $\rho_{c'} = \epsilon_\infty \cdot \rho_c$ and hence $\tau_{\rho_{c'}}(t) = \tau_{\rho_c}(-t)$. Thus for $\mathbb{Z}/2\mathbb{Z}$ -aligned M , to extract all possible Thurston norm information from the $\tau_\rho(t)$ it suffices to consider only the boundary obstruction classes $\{\sigma_0, \sigma_1\}$. Note that a lift of the holonomy representation will correspond to σ_1 or σ_3 for a $\mathbb{Z}/2\mathbb{Z}$ -aligned M by [Cal06].

In contrast, when M is $\mathbb{Z}/2\mathbb{Z}$ -askew, the class ϵ_∞ becomes 0 in $H^1(\partial M; \mathbb{Z}/2\mathbb{Z})$ and so all four boundary obstruction classes need to be considered when trying to understand the Thurston norm. Here, a lift of the holonomy representation will correspond to σ_1 or σ_2 . We now give two examples that illustrate a new behavior that can arise when M is $\mathbb{Z}/2\mathbb{Z}$ -askew: for the holonomy representation, the degree of $\tau_{2,\rho}(t)$ can depend on the choice of lift.

Example 5.3. Let M be the census manifold $t12835$ which is $\mathbb{Z}/2\mathbb{Z}$ -askew and has an ideal triangulation with 8 tetrahedra. Here $H_1(M) = \mathbb{Z} \oplus \mathbb{Z}/6\mathbb{Z}$ and $x(M) = 2$.

For the boundary obstruction class σ_1 , we find using [DGY] that there are two corresponding lifts of the holonomy representation. These are in the same Galois orbit and the abstract number field is $K = \mathbb{Q}(\zeta)$ where the minimal polynomial of ζ is $x^4 - x^2 + 1$; this is the cyclotomic field where ζ is a primitive 12th root of unity.

The \mathbb{C}^2 -torsion polynomial is

$$4(t^2 + t^{-2}) + (-13\zeta^3 + 9\zeta)(t + t^{-1}) + (-24\zeta^2 + 16)$$

which has degree 4 and so gives a sharp bound on $x(M)$ and shows that M is not fibered. (The embeddings of K that give lifts of the holonomy representation are $\zeta \mapsto e^{-\pi i/6}$ and $\zeta \mapsto -e^{-\pi i/6}$; here, the two representations differ by ϵ_∞ . The other two embeddings give lifts of the holonomy representation for the manifold with the opposite orientation.)

For the boundary obstruction class σ_2 , we also find two lifts of the holonomy representation (again differing by ϵ_∞) with the same K (of necessity) and choices of ζ . However, this time the \mathbb{C}^2 -torsion polynomial is:

$$(3\zeta^3 + 5\zeta)(t + t^{-1})$$

which has only degree 2 in t ! In particular, it is *not* the case that every lift of the holonomy representation gives a sharp bound on $x(M)$.

Example 5.4. Let M be the census manifold $o9_{43413}$ which is $\mathbb{Z}/2\mathbb{Z}$ -askew and has an ideal triangulation with 9 tetrahedra, $H_1(M; \mathbb{Z}) = \mathbb{Z} \oplus \mathbb{Z}/2$, and $x(M) = 4$.

For the boundary obstruction class σ_1 , we find there are two corresponding lifts of the holonomy representation. The field is $K = \mathbb{Q}(\omega)$ where the minimal polynomial of ω is $x^6 - x^2 + 1$, and the two relevant embeddings in are $\omega \approx \pm(0.87498455 + 0.32130825i)$. The \mathbb{C}^2 -torsion polynomial of these representations has degree 8:

$$4(t^4 + t^{-4}) + (-6\omega^4 + 3\omega^2 - 2)(t^2 + t^{-2}) + (20\omega^4 - 6\omega^2 - 12)$$

which gives a sharp bound on $x(M)$ and shows that M is not fibered. Whereas, for the boundary obstruction class σ_2 , we find the \mathbb{C}^2 -torsion is

$$(2\omega^4 + \omega^2 - 2)(t^2 + t^{-2}) + (-4\omega^5 - 4\omega^3 + 2\omega)(t + t^{-1}) + (4\omega^4 + 2\omega^2 - 4)$$

which has degree 4 in t (the two relevant embeddings in \mathbb{C} remain the same). At the same time, the field generated by the coefficients of the polynomial is now the whole trace field, whereas for the first polynomial it was an index-2 subfield.

5.6. Sharpness of torsion bounds on the Thurston norm. For our nonfibered manifolds, we find using [DGY] that:

Theorem 5.5. *For each of the 6,672 nonfibered hyperbolic manifolds above, there is at least one lift ρ of the holonomy representation where $x(M) = \frac{1}{2}\tau_{2,\rho}(t)$. Indeed, this is the case for all ρ corresponding to the boundary obstruction class σ_1 . In contrast, there are 50 manifolds (necessarily $\mathbb{Z}/2\mathbb{Z}$ -askew) where some lift corresponding to σ_2 has $x(M) > \frac{1}{2}\tau_{2,\rho}(t)$. Finally, for every lift of the holonomy representation $\tau_{2,\rho}(t)$ is nonmonic.*

A caveat is that $\tau_{2,\rho}(t)$ is nonmonic is “barely true” for $o9_{31518}$, where the leading coefficient is -1 ; recall from [DFJ12] that using the sign-refined torsion, the polynomial $\tau_{2,\rho}(t)$ is defined on the nose.

In contrast, the ordinary Alexander polynomial Δ_M does not detect $x(M)$ for 263 (3.9%) of these manifolds, and is monic for 212 (3.2%) of them (together, these amount to 362 (5.4%) manifolds). For the nonfibered knots looked at in [DFJ12], the analogous numbers were 8,834 (4.5%) and 7,972 (4.1%); thus the “interesting” portion of our sample is 25-30 times smaller than that of [DFJ12]. (There is no theorem that the \mathbb{C}^2 -torsion polynomial has to do at least as well as the basic Δ_M in either setting) The subset of $\mathbb{Z}/2\mathbb{Z}$ -askew manifolds where Δ_M does not detect $x(M)$ is just 56 manifolds (these include all 50 where some lift corresponding to σ_2 has $x(M) > \frac{1}{2}\tau_{2,\rho}(t)$). Given this, we are not so bold as to propose an analogue of Conjecture 5.2 for all 1-cusped hyperbolic 3-manifolds with $b_1(M) = 1$. Another natural question is to explain why lifts associated to σ_1 sometimes outperform those associated to σ_2 ; concretely, the former are those lifts ρ where $\text{tr}(\rho(\beta)) = -2$ for a \mathbb{Q} -longitude β .

REFERENCES

- [AD20] Ian Agol and Nathan Dunfield, *Certifying the Thurston norm via $SL(2, \mathbb{C})$ -twisted homology*, What’s next?—the mathematical legacy of William P. Thurston, Ann. of Math. Stud., vol. 205, Princeton Univ. Press, Princeton, NJ, 2020, pp. 1–20, doi:10.2307/j.ctvthhdv.4. MR4205633
- [Bel21] Mark Bell, *flipper (computer software)*, 2013–2021, Version 0.15.3, URL: <https://pypi.python.org/pypi/flipper>.
- [Bur] Benjamin A Burton, *The cusped hyperbolic census is complete*, Trans. Amer. Math. Soc., 34 pages, to appear, doi:10.1090/tran/6767.
- [But05] J. O. Button, *Fibred and virtually fibred hyperbolic 3-manifolds in the censuses*, Experiment. Math. **14** (2005), no. 2, 231–255. MR2169525
- [Cal06] Danny Calegari, *Real places and torus bundles*, Geom. Dedicata **118** (2006), 209–227, doi:10.1007/s10711-005-9037-9. MR2239457 (2007d:57026)
- [CDGW] Marc Culler, Nathan Dunfield, Matthias Goerner, and Jeffrey Weeks, *SnapPy, a computer program for studying the geometry and topology of 3-manifolds*, Version 3.1, 2023, URL: <http://snappy.computop.org>.

- [Cul86] Marc Culler, *Lifting representations to covering groups*, Adv. in Math. **59** (1986), no. 1, 64–70, [doi:10.1016/0001-8708\(86\)90037-X](https://doi.org/10.1016/0001-8708(86)90037-X). MR825087 (87g:22009)
- [DFJ12] Nathan Dunfield, Stefan Friedl, and Nicholas Jackson, *Twisted Alexander polynomials of hyperbolic knots*, Exp. Math. **21** (2012), no. 4, 329–352, [doi:10.1080/10586458.2012.669268](https://doi.org/10.1080/10586458.2012.669268). MR3004250
- [DFJ20] ———, *Twisted Alexander polynomials for hyperbolic knots: data and software*, 2020, [doi:10.7910/DVN/OK6YGC](https://doi.org/10.7910/DVN/OK6YGC).
- [DG12] Nathan Dunfield and Stavros Garoufalidis, *Incompressibility criteria for spun-normal surfaces*, Trans. Amer. Math. Soc. **364** (2012), no. 11, 6109–6137, [doi:10.1090/S0002-9947-2012-05663-7](https://doi.org/10.1090/S0002-9947-2012-05663-7). MR2946944
- [DG13] Tudor Dimofte and Stavros Garoufalidis, *The quantum content of the gluing equations*, Geom. Topol. **17** (2013), no. 3, 1253–1315, [doi:10.2140/gt.2013.17.1253](https://doi.org/10.2140/gt.2013.17.1253). MR3073925
- [DGY] Nathan M. Dunfield, Stavros Garoufalidis, and Seokbeom Yoon, *Code and data for comparing 1-loop invariants and torsions*, Harvard Dataverse, [doi:10.7910/DVN/XUJ3RH](https://doi.org/10.7910/DVN/XUJ3RH).
- [Dun20] Nathan M. Dunfield, *A census of exceptional Dehn fillings*, Characters in low-dimensional topology, Contemp. Math., vol. 760, Amer. Math. Soc., 2020, pp. 143–155, [doi:10.1090/comm/760/15289](https://doi.org/10.1090/comm/760/15289). MR4193924
- [FH82] William Floyd and Alan Hatcher, *Incompressible surfaces in punctured-torus bundles*, Topology Appl. **13** (1982), no. 3, 263–282, [doi:10.1016/0166-8641\(82\)90035-9](https://doi.org/10.1016/0166-8641(82)90035-9). MR651509
- [Fri88] David Fried, *Counting circles*, Dynamical systems (College Park, MD, 1986–87), Lecture Notes in Math., vol. 1342, Springer, Berlin, 1988, pp. 196–215, [doi:10.1007/BFb0082832](https://doi.org/10.1007/BFb0082832). MR970556
- [GGZ15a] Stavros Garoufalidis, Matthias Goerner, and Christian Zickert, *Gluing equations for $\mathrm{PGL}(n, \mathbb{C})$ -representations of 3-manifolds*, Algebr. Geom. Topol. **15** (2015), no. 1, 565–622, [doi:10.2140/agt.2015.15.565](https://doi.org/10.2140/agt.2015.15.565). MR3325748
- [GGZ15b] ———, *The Ptolemy field of 3-manifold representations*, Algebr. Geom. Topol. **15** (2015), no. 1, 371–397, [doi:10.2140/agt.2015.15.371](https://doi.org/10.2140/agt.2015.15.371). MR3325740
- [Goe] Matthias Goerner, *Unhyperbolic*, www.unhyperbolic.org.
- [GTZ15] Stavros Garoufalidis, Dylan Thurston, and Christian Zickert, *The complex volume of $\mathrm{SL}(n, \mathbb{C})$ -representations of 3-manifolds*, Duke Math. J. **164** (2015), no. 11, 2099–2160, [doi:10.1215/00127094-3121185](https://doi.org/10.1215/00127094-3121185). MR3385130
- [GYa] Stavros Garoufalidis and Seokbeom Yoon, *Super-representations of 3-manifolds and torsion polynomials*, Preprint 2023, [arXiv:2301.11018](https://arxiv.org/abs/2301.11018).
- [GYb] ———, *Twisted Neumann–Zagier matrices*, Preprint 2021, [arXiv:2109.00379](https://arxiv.org/abs/2109.00379).
- [Hat91] Allen Hatcher, *On triangulations of surfaces*, Topology Appl. **40** (1991), no. 2, 189–194, [doi:10.1016/0166-8641\(91\)90050-V](https://doi.org/10.1016/0166-8641(91)90050-V). MR1123262
- [HRST15] Craig Hodgson, J. Hyam Rubinstein, Henry Segerman, and Stephan Tillmann, *Triangulations of 3-manifolds with essential edges*, Ann. Fac. Sci. Toulouse Math. (6) **24** (2015), no. 5, 1103–1145, [doi:10.5802/afst.1477](https://doi.org/10.5802/afst.1477). MR3485328
- [Kit96] Teruaki Kitano, *Twisted Alexander polynomial and Reidemeister torsion*, Pacific J. Math. **174** (1996), no. 2, 431–442. MR1405595
- [Lac00] Marc Lackenby, *Taut ideal triangulations of 3-manifolds*, Geom. Topol. **4** (2000), 369–395, [doi:10.2140/gt.2000.4.369](https://doi.org/10.2140/gt.2000.4.369). MR1790190
- [LMT] Michael Landry, Yair Minsky, and Samuel Taylor, *A polynomial invariant for veering triangulations*, Preprint 2020, [arXiv:2008.04836](https://arxiv.org/abs/2008.04836).
- [McM00] Curtis McMullen, *Polynomial invariants for fibered 3-manifolds and Teichmüller geodesics for foliations*, Ann. Sci. École Norm. Sup. (4) **33** (2000), no. 4, 519–560, [doi:10.1016/S0012-9593\(00\)00121-X](https://doi.org/10.1016/S0012-9593(00)00121-X). MR1832823
- [Par] Anna Parlak, *The taut polynomial and the Alexander polynomial*, Preprint 2021, [arXiv:2101.12162](https://arxiv.org/abs/2101.12162).
- [Sik12] Adam Sikora, *Character varieties*, Trans. Amer. Math. Soc. **364** (2012), no. 10, 5173–5208, [doi:10.1090/S0002-9947-2012-05448-1](https://doi.org/10.1090/S0002-9947-2012-05448-1). MR2931326

- [Wad94] Masaaki Wada, *Twisted Alexander polynomial for finitely presentable groups*, *Topology* **33** (1994), no. 2, 241–256, [doi:10.1016/0040-9383\(94\)90013-2](https://doi.org/10.1016/0040-9383(94)90013-2). [MR1273784](#)
- [Wei64] André Weil, *Remarks on the cohomology of groups*, *Ann. of Math. (2)* **80** (1964), 149–157, [doi:10.2307/1970495](https://doi.org/10.2307/1970495). [MR169956](#)
- [Yam08] Yoshikazu Yamaguchi, *A relationship between the non-acyclic Reidemeister torsion and a zero of the acyclic Reidemeister torsion*, *Ann. Inst. Fourier (Grenoble)* **58** (2008), no. 1, 337–362. [MR2401224](#)
- [Yoo] Seokbeom Yoon, *The twisted 1-loop invariant and the Jacobian of ptolemy coordinates*, Preprint 2021, [arXiv:2110.11003](https://arxiv.org/abs/2110.11003).
- [Yoo19] ———, *The volume and Chern-Simons invariant of a Dehn-filled manifold*, *Topology Appl.* **256** (2019), 208–227, [doi:10.1016/j.topol.2019.02.004](https://doi.org/10.1016/j.topol.2019.02.004). [MR3913118](#)

UNIVERSITY OF ILLINOIS URBANA-CHAMPAIGN, DEPT. OF MATHEMATICS, URBANA, IL 61801, USA

Email address: nathan@dunfield.info

URL: <https://dunfield.info>

INTERNATIONAL CENTER FOR MATHEMATICS, DEPARTMENT OF MATHEMATICS, SOUTHERN UNIVERSITY OF SCIENCE AND TECHNOLOGY, SHENZHEN, CHINA

Email address: stavros@mpim-bonn.mpg.de

URL: <http://people.mpim-bonn.mpg.de/stavros>

INTERNATIONAL CENTER FOR MATHEMATICS,, SOUTHERN UNIVERSITY OF SCIENCE AND TECHNOLOGY, SHENZHEN, CHINA

Email address: sbyoon15@gmail.com

URL: <http://sites.google.com/view/seokbeom>